Electronic Supplementary Material (ESI) for Dalton Transactions.

Supplementary Materials for

Cobalt Schiff-Base Complexes for Electrocatalytic Hydrogen Generation

Ryan J. DiRisio, Jessica E. Armstrong, Mariah A. Frank, William R. Lake, and William R. McNamara
Correspondence to: wrmcnamara@wm.edu

Table of Contents

Supplementary Text:

Back calculations of i_c/i_p:

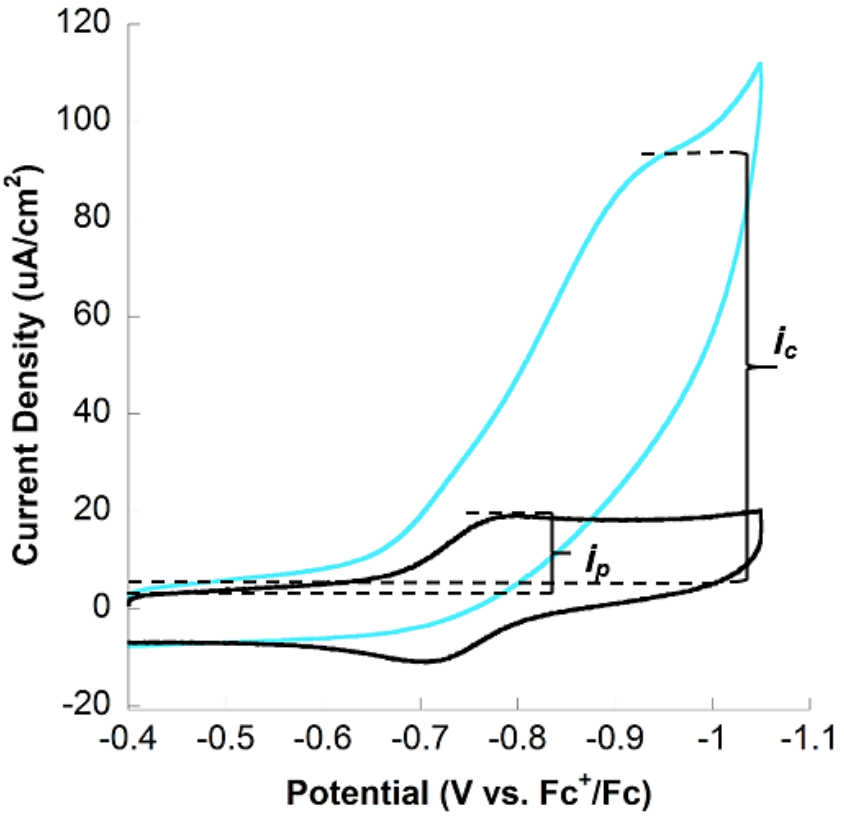

Figure S1. Experimental determination of i_c/i_p. CVs of 0.1 M $TBAPF_6$ in CH_3CN (black), and an addition of 0.88 mM TFA (blue).[1]

To back calculate i_c/i_p, the following equation is used:[2]

$$\frac{i_c}{i_p} = \frac{\mathrm{n}}{0.4463}\sqrt{\frac{\mathrm{RT}k_{\mathrm{cat}}[\mathrm{H}^+]}{\mathrm{F}\nu}}$$

Where n is the number of electrons involved in the proton reduction process, R is the universal gas constant (J/(mol×K)), T is temperature (K), $[H^+]$ is the bulk concentration of protons in solution (M^{-1}), F is the faraday constant (C/mol), and ν is the scan rate (V/s).[2,3] The k_{cat} values from FOWA calculations were used to back calculate i_c/i_p for the determination of the rate-determining step (see Fig. S17 and Fig. 8).

Calculation of k_{cat} from FOWA:

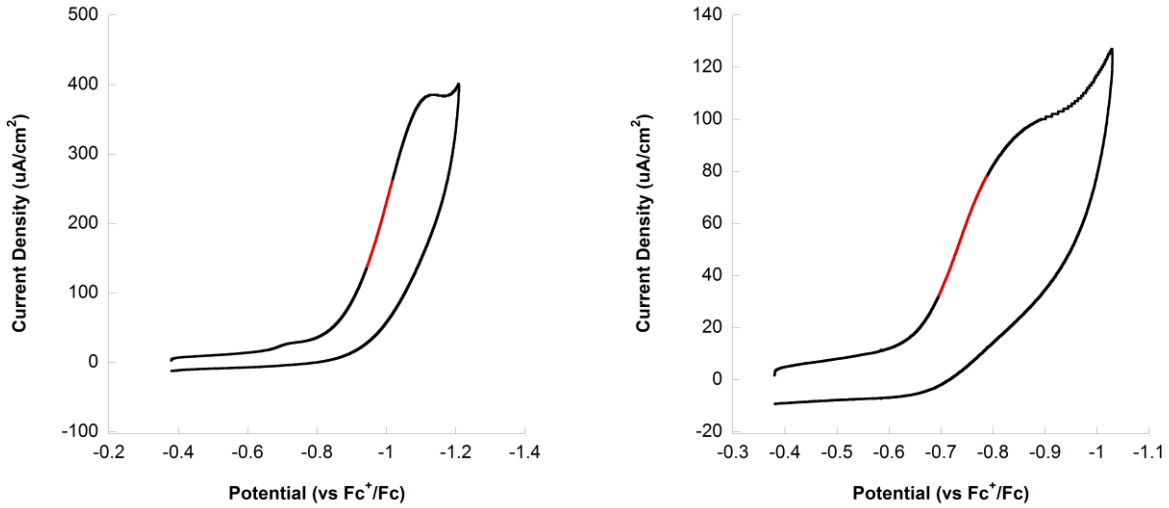

Figure S2. Portions (in red) of the catalytic current response of **2** (left) and **3** (right) used for FOWA. This region represents the largest linear portion of the foot-of-the-wave.[5]

For **2** and **3**, the catalytic response does not display ideal behavior.[2,3] This is due to many factors, including proton consumption, and catalyst decomposition.[3] Therefore, traditional k_{obs} calculations provide a non-ideal representation of the catalytic activity of **2** and **3**. To more accurately describe the ideal activity, foot-of-the-wave analysis (FOWA) has been developed by Savéant and coworkers.[4] For an EECC and ECEC process, current is represented:[3]

$$i = \frac{2\mathrm{FAC_p^0}\sqrt{\mathrm{D}k_{obs}}}{1 + \mathrm{e}^{\left[\frac{\mathrm{F}}{\mathrm{RT}}(\mathrm{E}-\mathrm{E_{cat/2}})\right]}}$$

Where i is current density (A/cm^2), F is the Faraday constant (C/mol), A is the surface area of the electrode (cm^2), C_p^0 is the bulk concentration of catalyst in solution (M), D is the diffusion coefficient (cm^2/s), and k_{obs} is the rate constant (s^{-1}). The Randles-Sevcik equation describes the peak current of a reversible catalytic wave:[4]

$$i_p = 0.4463\mathrm{FAC_p^0}\sqrt{\frac{\mathrm{F\nu D}}{\mathrm{RT}}}$$

Dividing i by i_p yields the equation:

$$\frac{i}{i_p} = \frac{2\sqrt{\frac{\mathrm{RT}}{\mathrm{F\nu}}}\sqrt{\mathrm{k_{obs}}}}{0.4463} * \frac{1}{1 + \mathrm{e}^{\left[\frac{\mathrm{F}}{\mathrm{RT}}(\mathrm{E}-\mathrm{E_{cat/2}})\right]}}$$

$\frac{i}{i_p}$ is then plotted vs. $\frac{1}{1+e^{\left[\frac{F}{RT}\left(E-E_{cat/2}\right)\right]}}$ to yield a line with a slope of $m = \frac{2\sqrt{\frac{RT}{Fv}}\sqrt{k_{obs}}}{0.4463}$, see Figure S3. From this slope, a k_{obs} value can be calculated.[3]

$$k_{obs} = \frac{(m^2)(0.4463)^2 Fv}{4RT}$$

This equation describes the kinetic activity obtained from the ideal foot of the wave. Figure S2 highlights the measured portion of the wave in which this takes place. From the k_{obs} value, which is in units s^{-1}, one can retrieve a catalytic rate constant by dividing by the concentration of acid in the cell. This yields a k_{cat} value in $M^{-1}s^{-1}$:

$$k_{cat} = \frac{k_{obs}}{[H^+]}$$

If k_{cat} is determined to be the rate determining step, a theoretical maximum turnover frequency (TOF_{max}) is calculated by multiplying k_{cat} by 1 M acid.[3] In addition, an experimental TOF value is calculated by multiplying k_{cat} by the bulk concentration of acid in the cell.

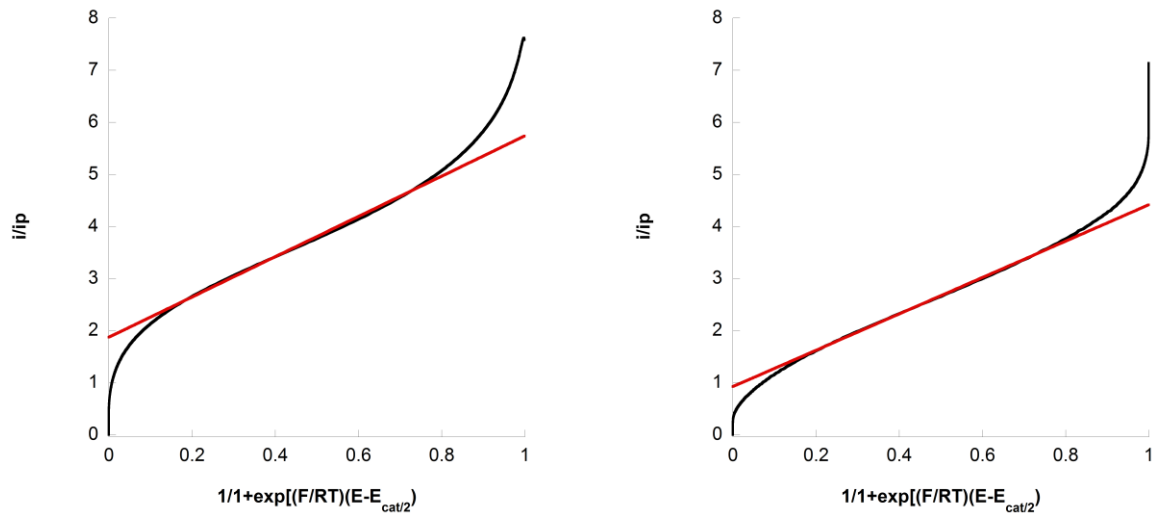

Figure S3. Linear fit for FOWA for **2** (left), R^2=0.996, and **3** (right), R^2=0.999.

Sample Calculation of k_{cat} of 2 at ν = 200 mv/s from FOWA:

$$k_{obs} = \frac{(\mathrm{m}^2)(0.4463)^2 \mathrm{F} \nu}{4\mathrm{RT}}$$

$$k_{obs} = \frac{(3.883^2)(0.4463)^2 * 96485 \frac{\mathrm{C}}{\mathrm{mol}} * 0.2 \frac{\mathrm{V}}{\mathrm{s}}}{4 * 8.314 \frac{\mathrm{J}}{\mathrm{mol} * \mathrm{K}} * 298\ \mathrm{K}}$$

$$\boldsymbol{k_{obs} = 5.85\ s^{-1}}$$

$$k_{cat} = \frac{k_{obs}}{[H^+]}$$

$$\boldsymbol{k_{cat} = \frac{5.85\ s^{-1}}{0.003\ M} = 1898\ M^{-1}s^{-1}}$$

Determination of Overpotential:

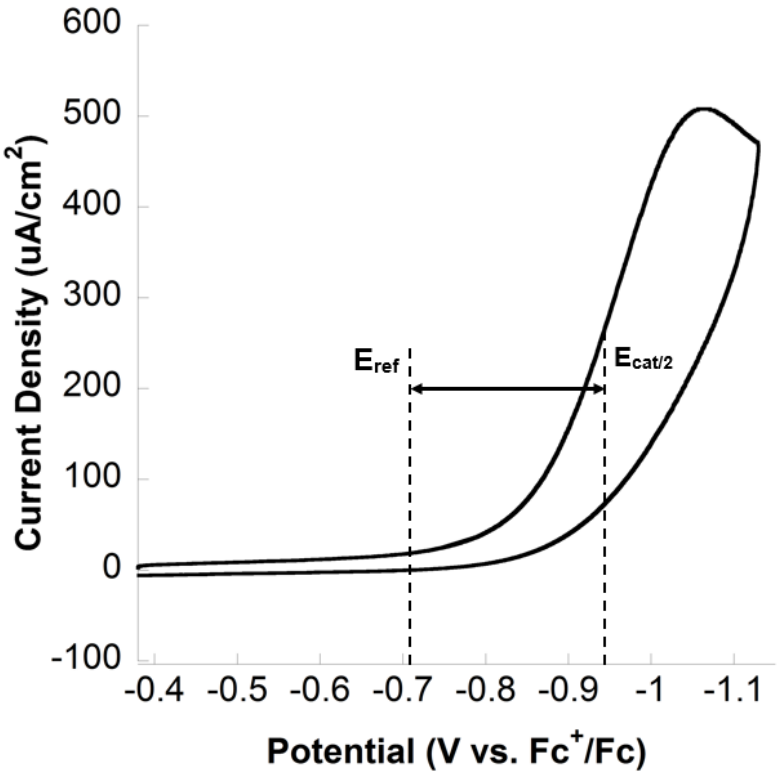

Figure S4. Overpotential is determined by the difference between the half wave potential of the irreversible catalytic event and the E_{ref} for the acid.[1]

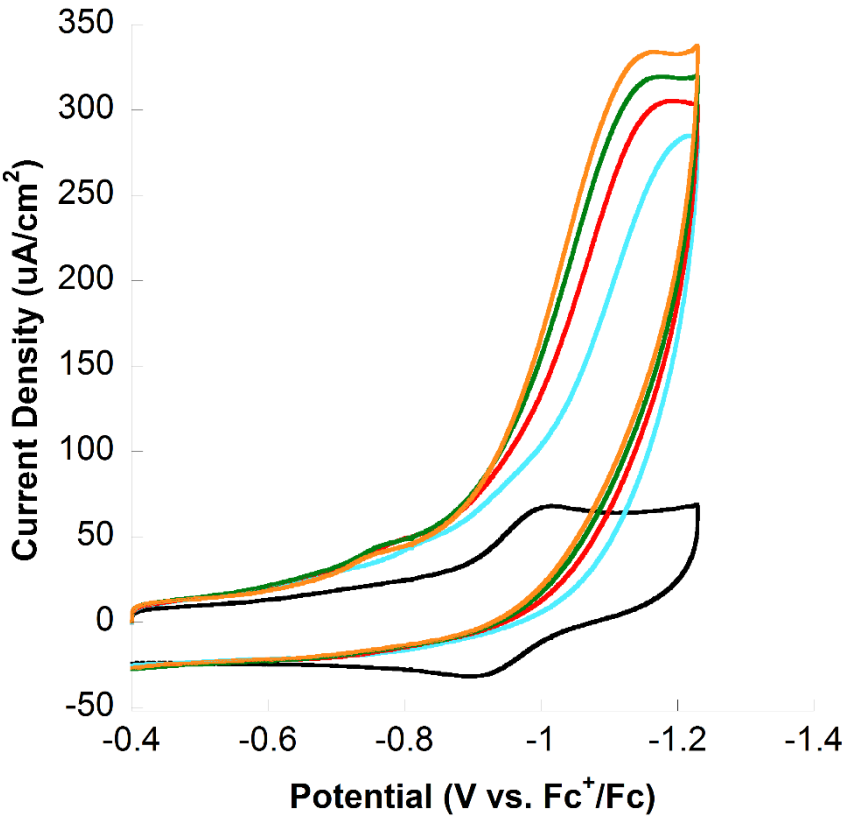

Figure S5. CV of 0 mM (Black), 0.77 mM (Blue), 1.54 mM (Red), 2.31 mM (Green), 3.08 mM (Orange) of TFA with 0.5 mg of **2** and 0.1 M $TBAPF_6$ at v = 500 mV/s in CH_3CN.

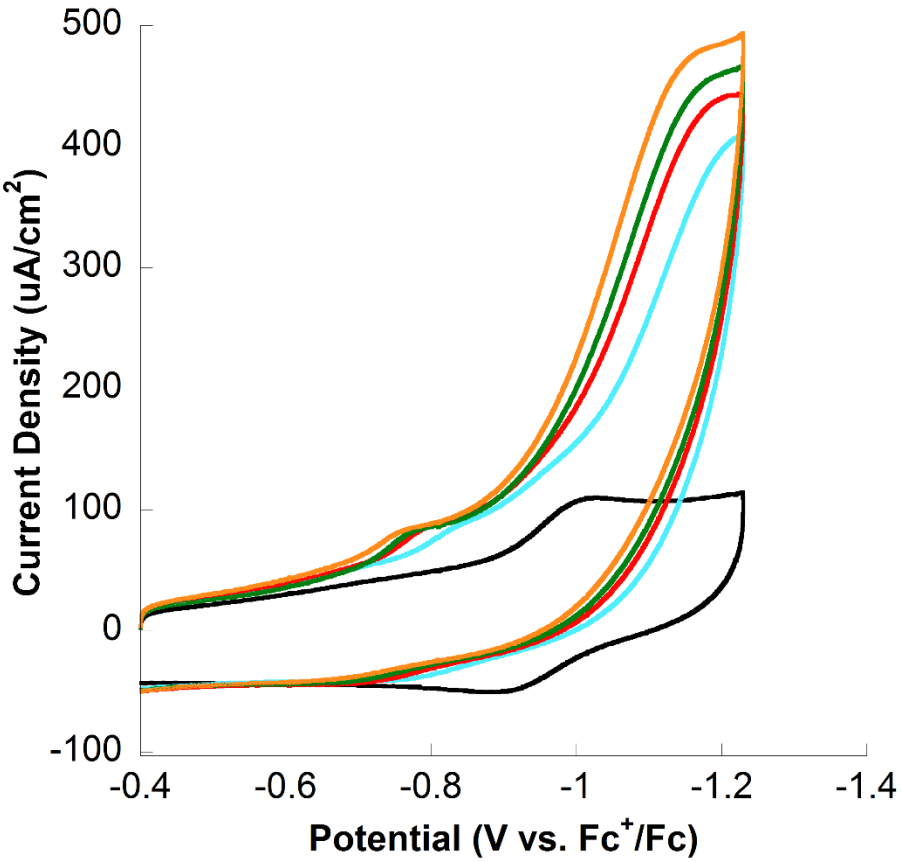

Figure S6. CV of 0 mM (Black), 0.77 mM (Blue), 1.54 mM (Red), 2.31 mM (Green), 3.08 mM (Orange) of TFA with 0.5 mg of **2** and 0.1 M $TBAPF_6$ at ν = 1 V/s in CH_3CN.

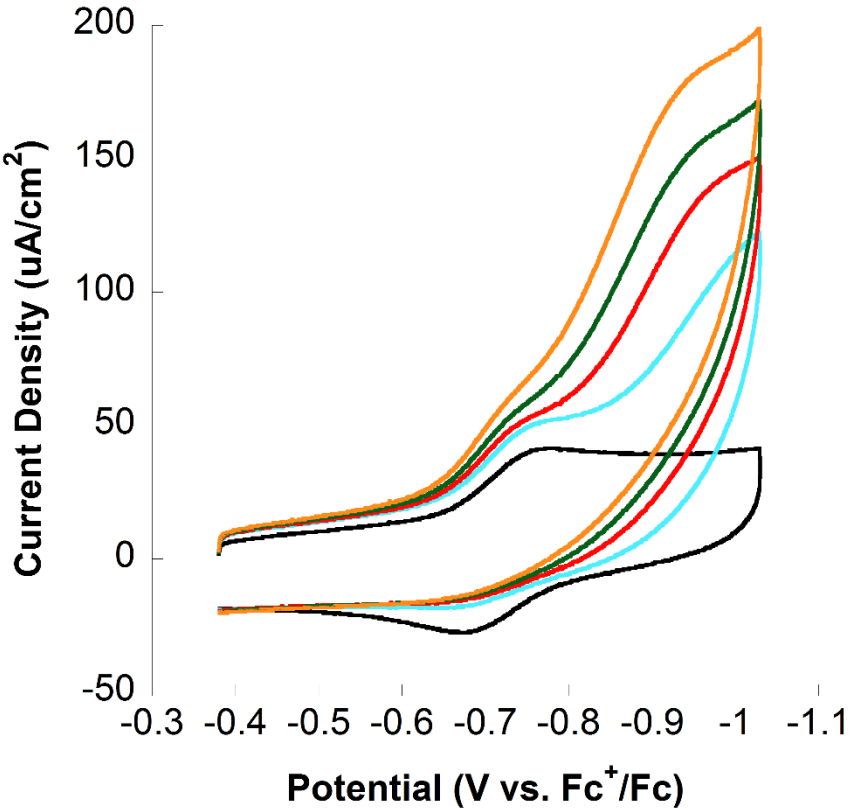

Figure S7. CV of 0 mM (Black), 0.22 mM (Blue), 0.44 mM (Red), 0.66 mM (Green), and 0.88 mM (Orange) of TFA with 0.5 mg of **3** and 0.1 M $TBAPF_6$ at ν = 600 mV/s in CH_3CN.

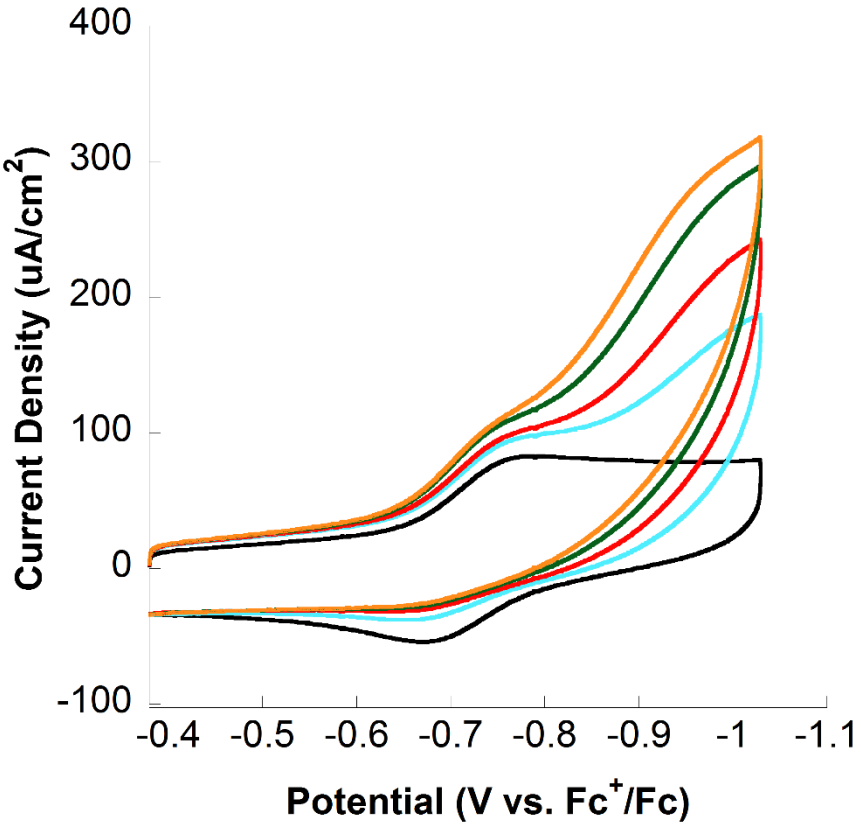

Figure S8. CV of 0 mM (Black), 0.22 mM (Blue), 0.44 mM (Red), 0.66 mM (Green), and 0.88 mM (Orange) of TFA with 0.5 mg of **3** and 0.1 M $TBAPF_6$ at ν = 1 V/s in CH_3CN.

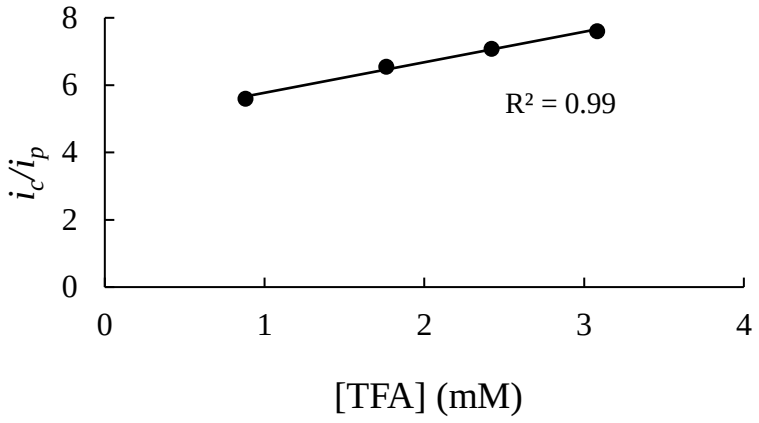

Figure S9. The i_c/i_p vs. [TFA] for CVs of 0.5 mg of **2** in CH_3CN with 0.1 M $TBAPF_6$ upon addition of 0.88 mM, 1.76 mM, 2.42 mM, and 3.08 mM TFA at v = 200 mV/s was fit with a linear correlation. It is important to note that this is a narrow range of [TFA] and that i_c/i_p vs [TFA] deviates from linearity at higher acid concentration where catalyst decomposition is observed.

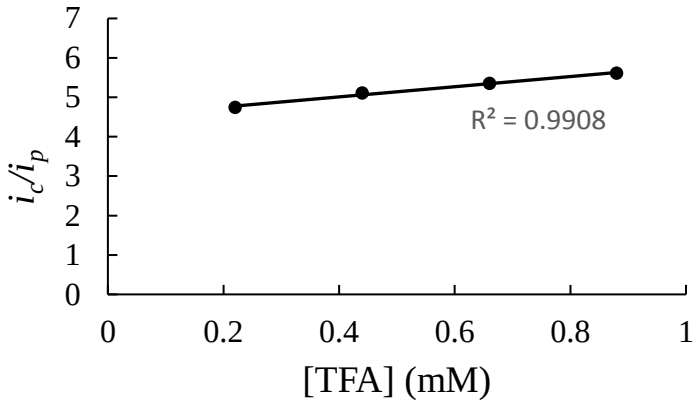

Figure S10. The i_c/i_p vs. [TFA] for CVs of 0.5 mg of **3** in CH_3CN with 0.1 M $TBAPF_6$ upon addition of 0.22 mM, 0.44 mM, 0.66 mM, and 0.88 mM TFA at v = 200 mV/s was fit with a linear correlation. It is important to note that this is a narrow range of [TFA] and that i_c/i_p vs [TFA] deviates from linearity at higher acid concentration where catalyst decomposition is observed.

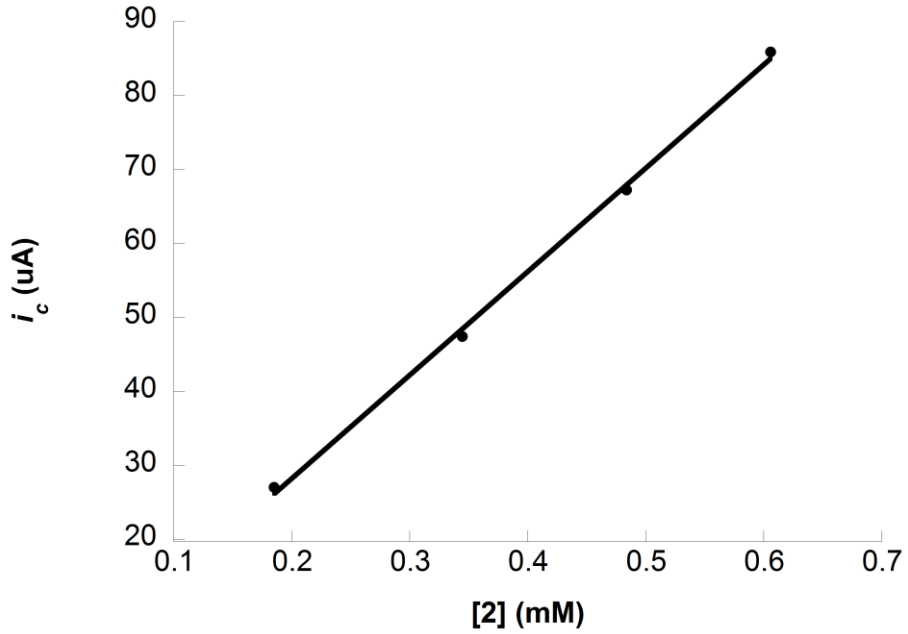

Figure S11. The i_c vs. [**2**] for CVs of ferrocene and 44 mM TFA in 5 mL of 0.1 M $TBAPF_6$ in CH_3CN without **2** added and upon the addition of 0.2 mM, 0.4 mM, 0.6 mM, and 0.8 mM of **2** at v = 200 mV/s was fit with a linear correlation.

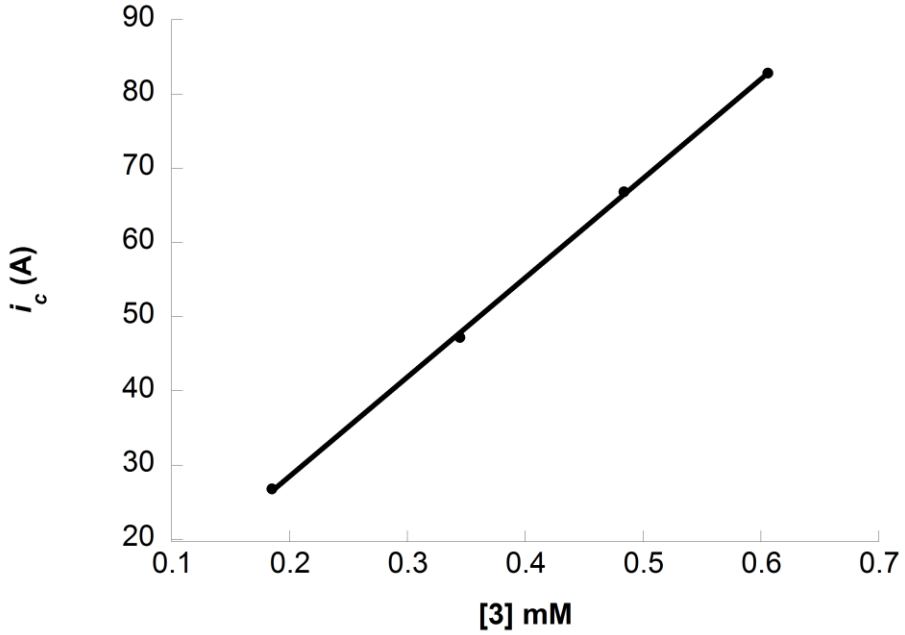

Figure S12. The i_c vs. [**3**] for CVs of ferrocene and 44 mM TFA in 5 mL of 0.1 M $TBAPF_6$ in CH_3CN without **3** added and upon the addition of 0.2 mM, 0.4 mM, 0.6 mM, and 0.8 mM of **3** at v = 200 mV/s was fit with a linear correlation.

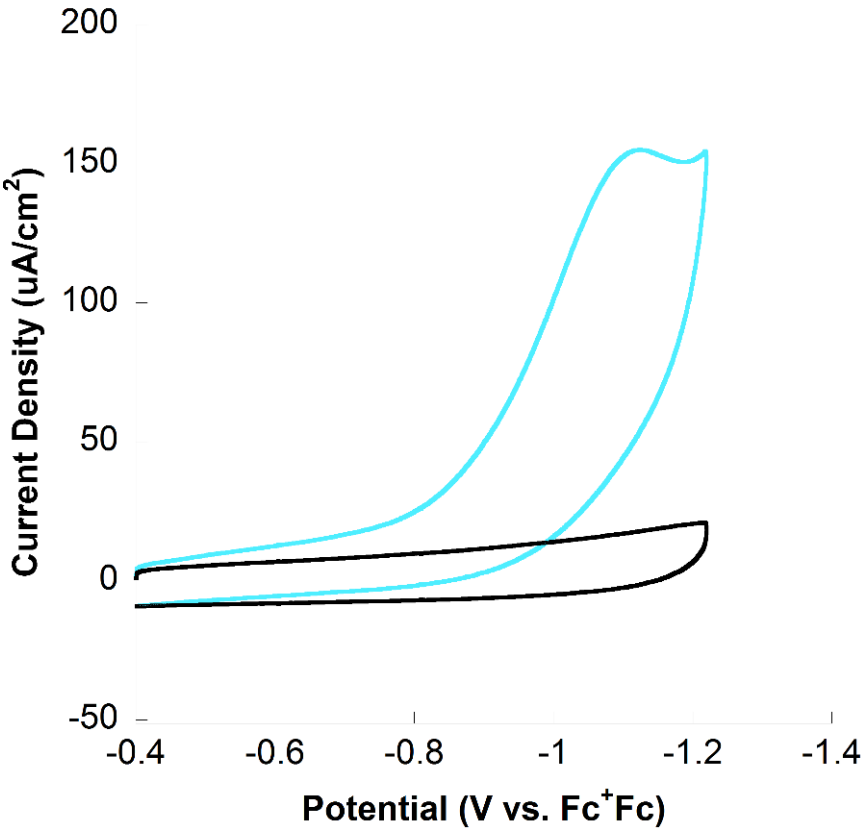

Figure S13. Dip test: CVs with 8.8 mM of TFA with 0.5 mg **2** (Blue) in CH_3CN with 0.1 M $TBAPF_6$. The electrodes were then placed in a solution with CH_3CN and $TBAPF_6$ (Black). v = 200 mV/s.

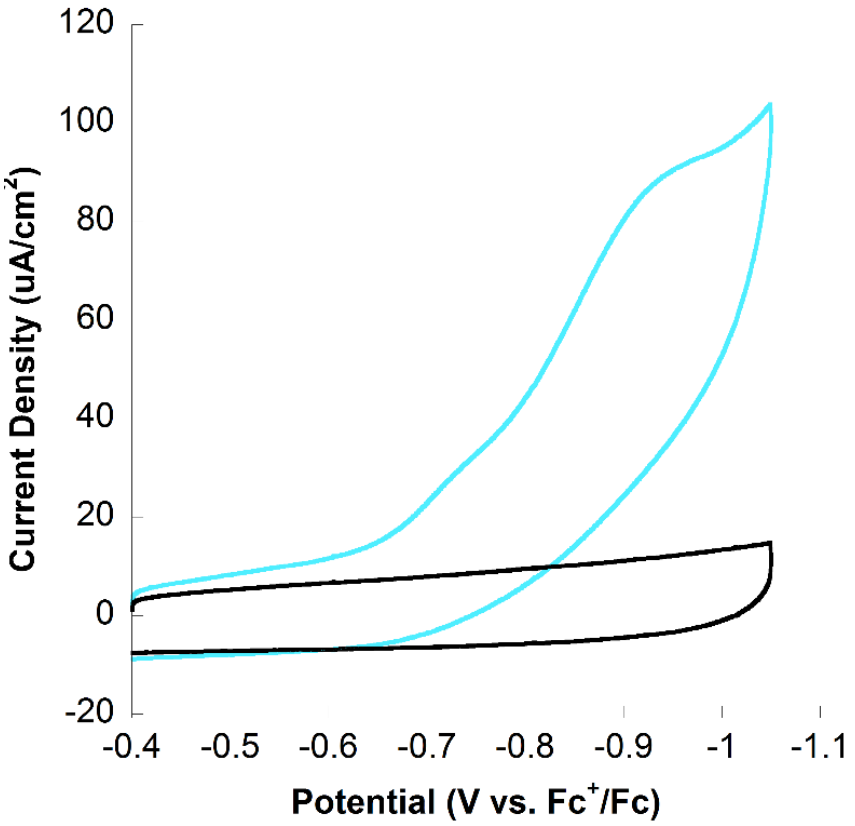

Figure S14. Dip test: CVs with 8.8 mM of TFA and 0.5 mg of **3** (Blue) in CH_3CN with 0.1 M $TBAPF_6$. The electrodes were then placed in a solution with CH_3CN and $TBAPF_6$ (Black). v = 200 mV/s.

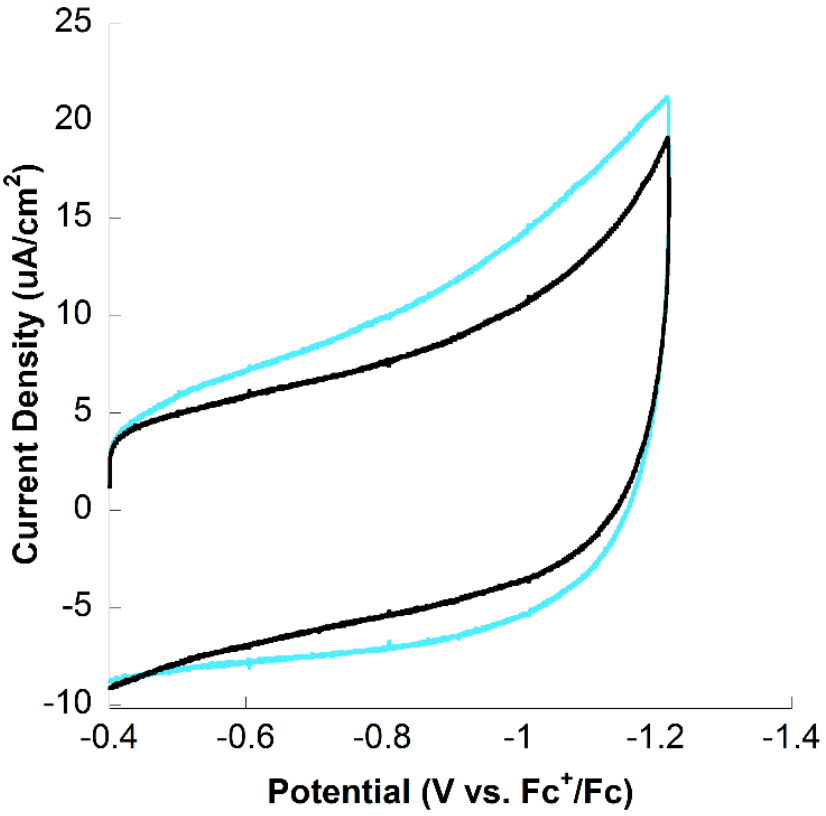

Figure S15. CVs of 0.1 M $TBAPF_6$ in CH_3CN without TFA (Black) and addition of 13.2 mM TFA (Blue) in the range of **2**.

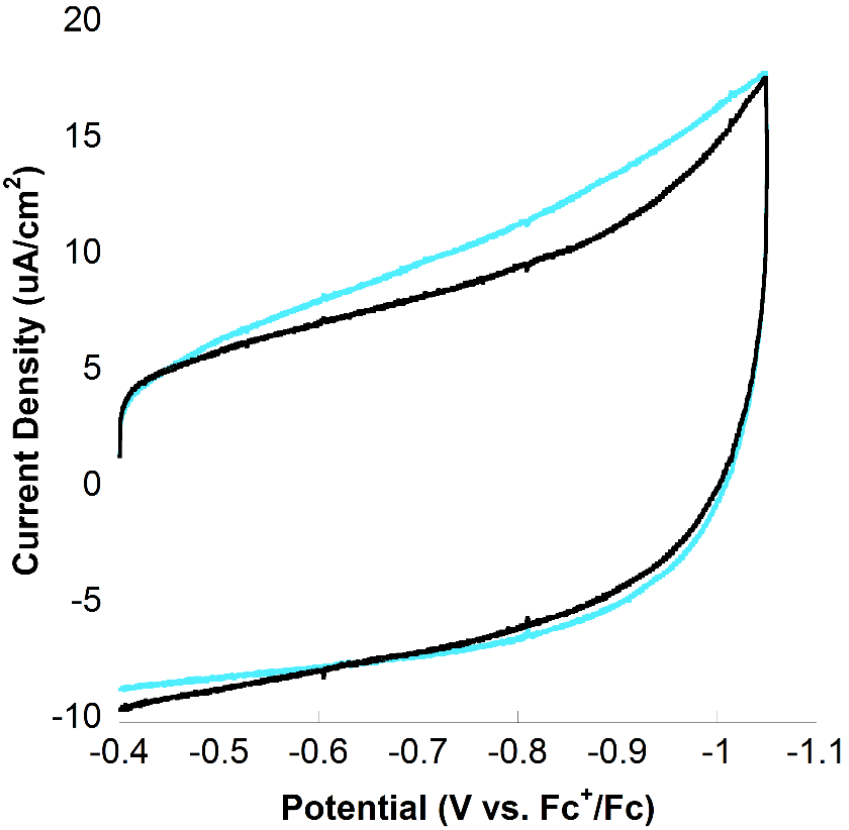

Figure S16. CVs of 0.1 M $TBAPF_6$ in CH_3CN without TFA (Black) and addition of 13.2 mM TFA (Blue) in the range of **3**.

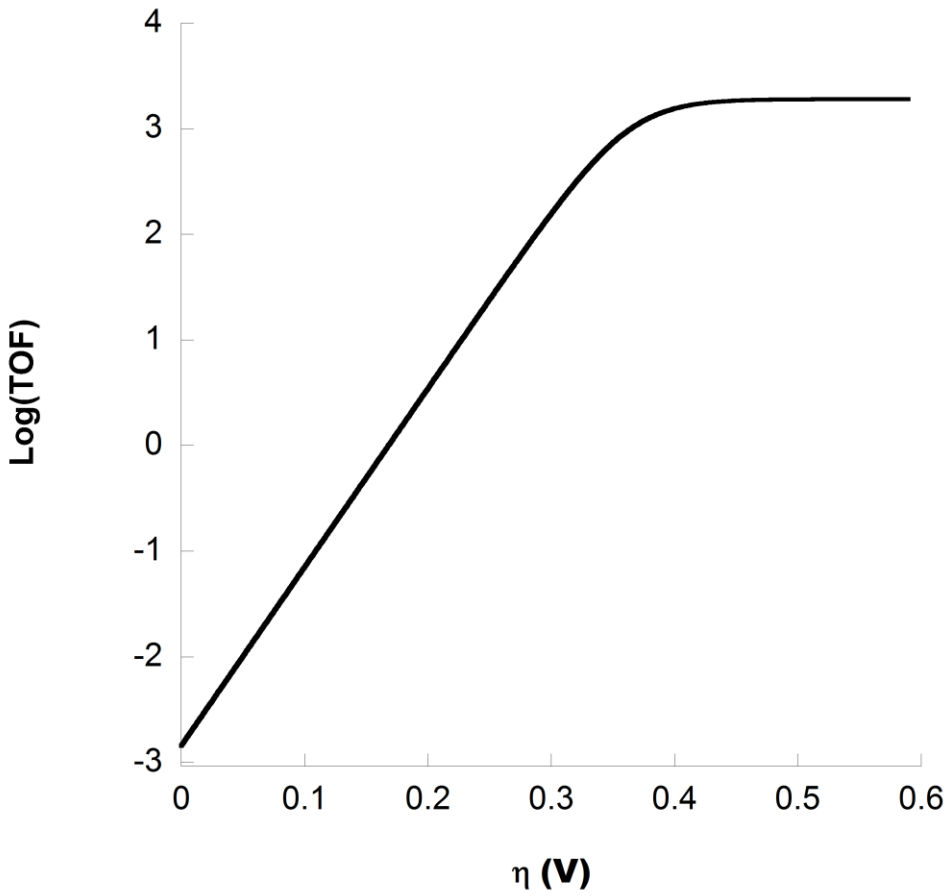

Figure S17. Tafel plot of **2** at ν = 200 mV/s.

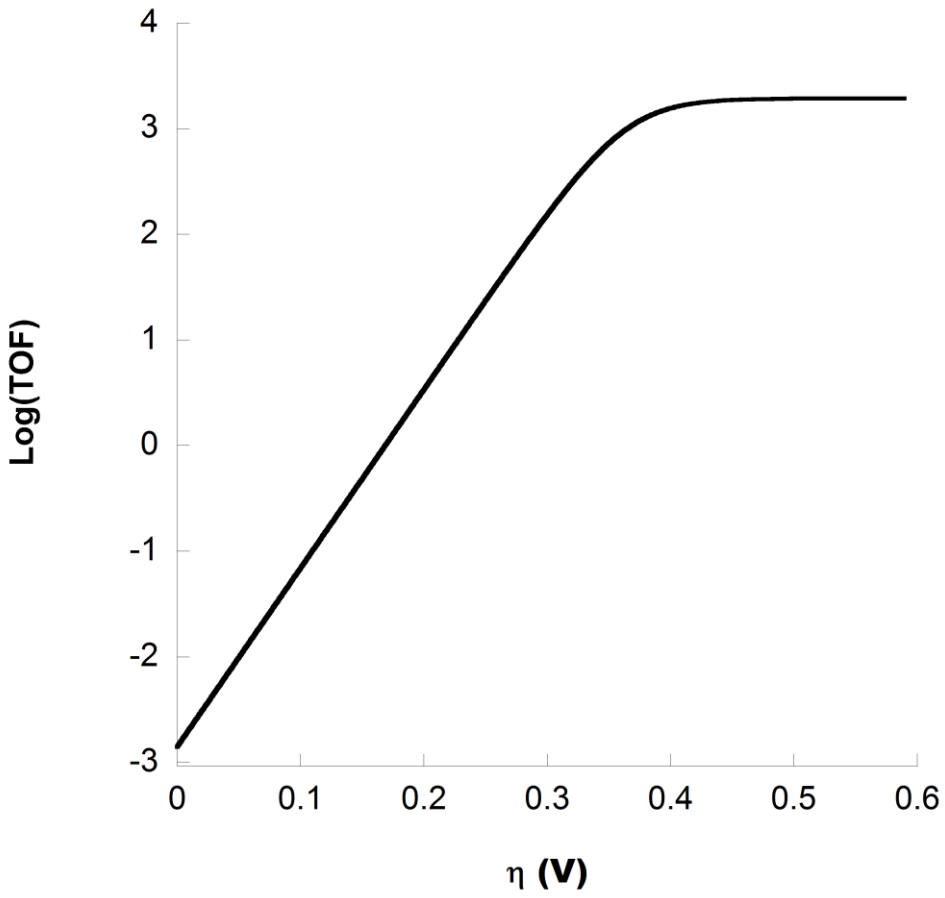

Figure S18. Tafel plot of **2** at ν = 500 mV/s.

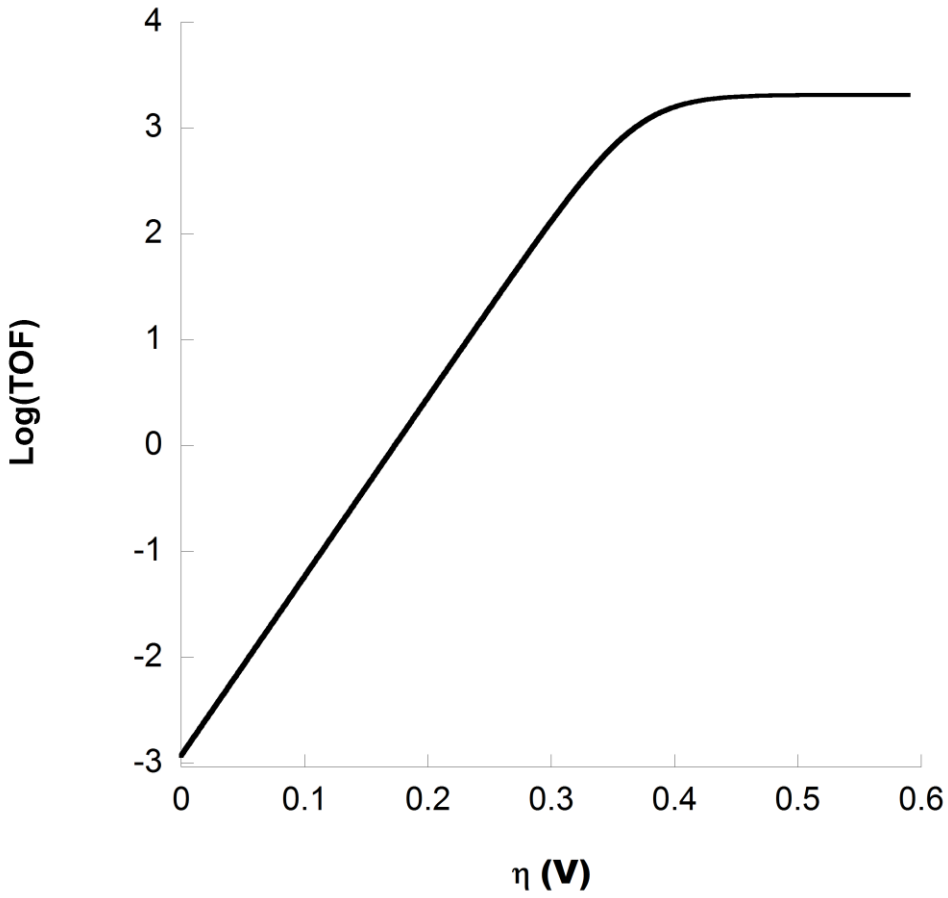

Figure S19. Tafel plot of **2** at ν = 1 V/s.

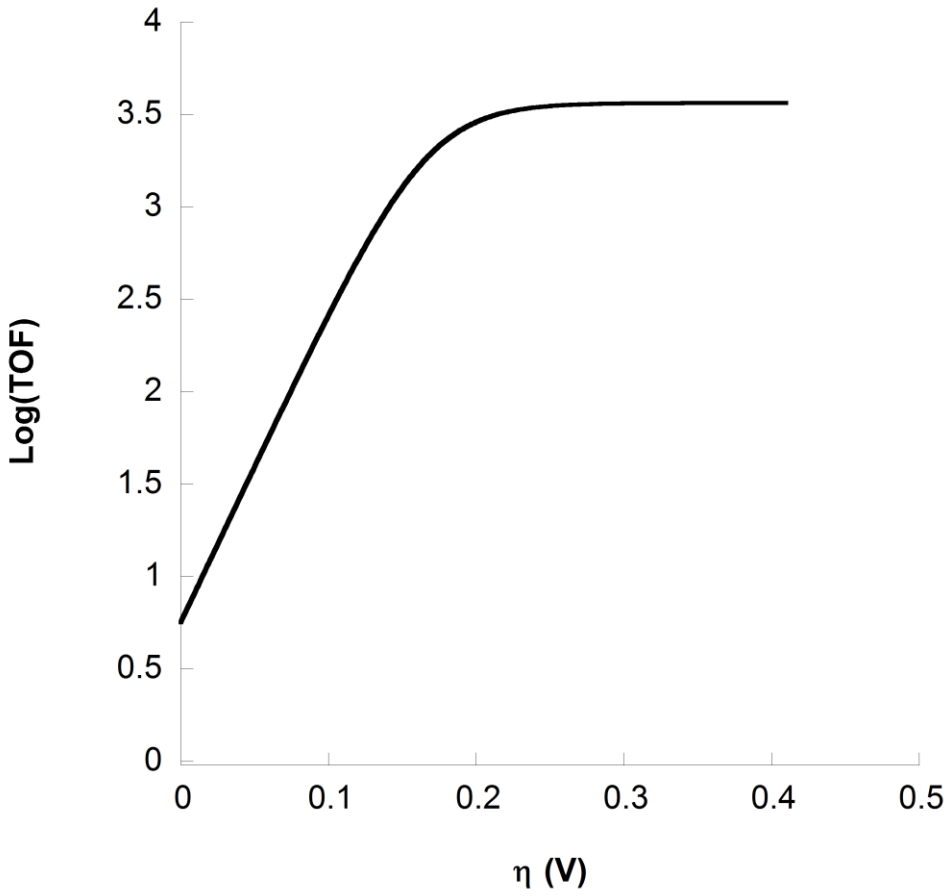

Figure S20. Tafel plot of **3** at ν = 200 mV/s.

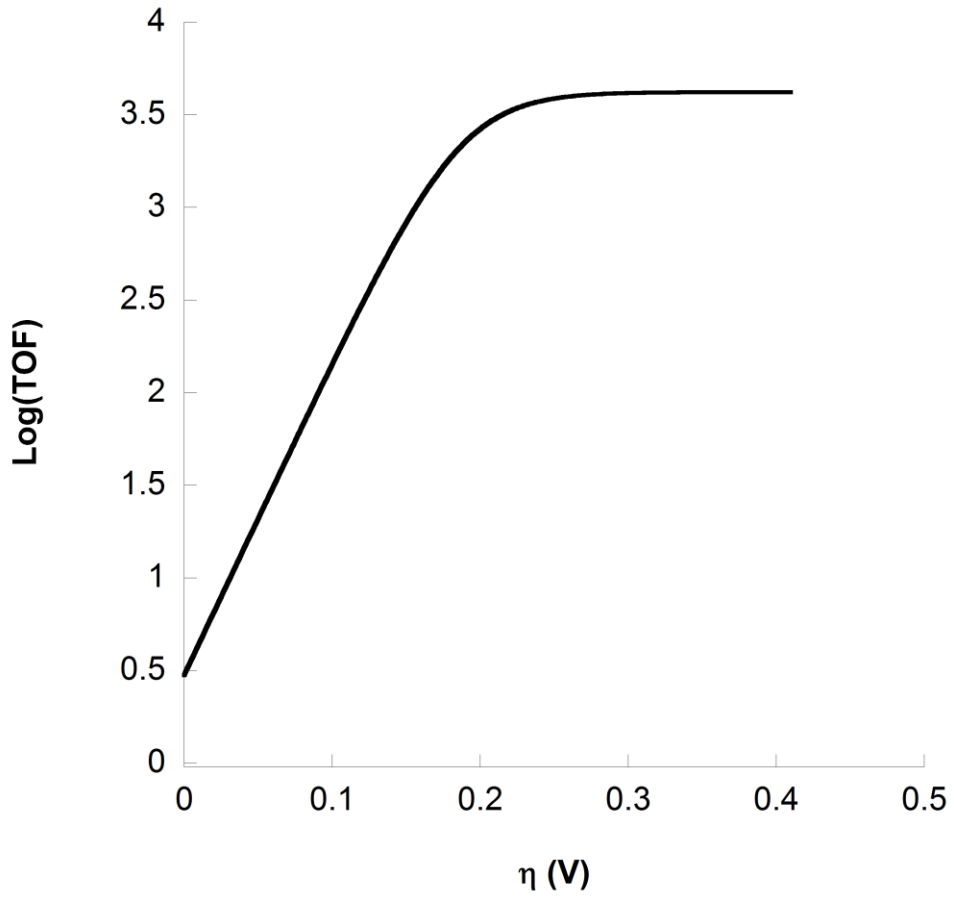

Figure S21. Tafel plot of **3** at ν = 600 mV/s.

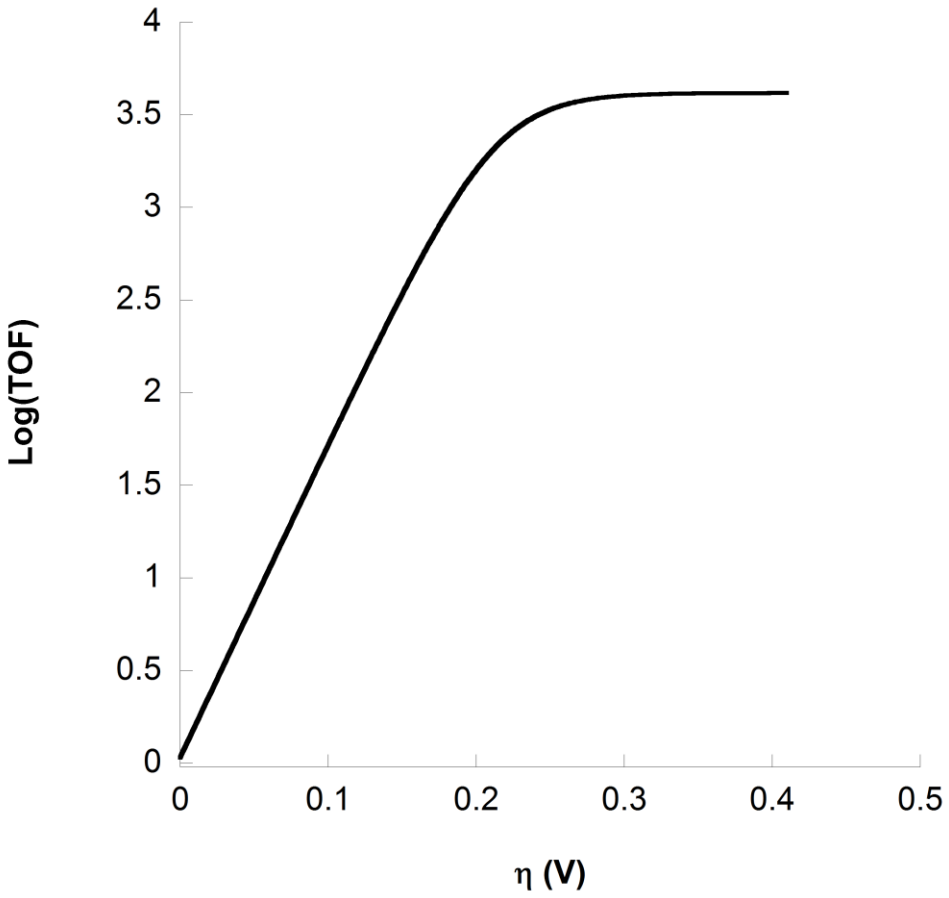

Figure S22. Tafel plot of **3** at ν = 1 V/s.

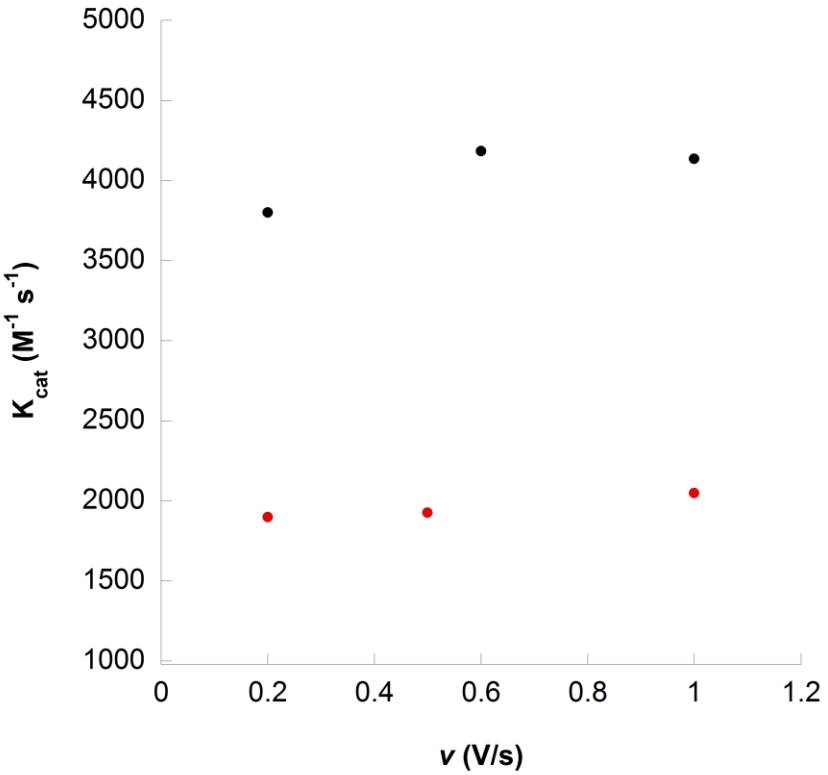

Figure S23. k_{cat} values for **2** (black) and **3** (red) at different scan rates. For complex **2** and **3**, k_{cat} levels off between ν = 600 mV/s and 1 V/s.

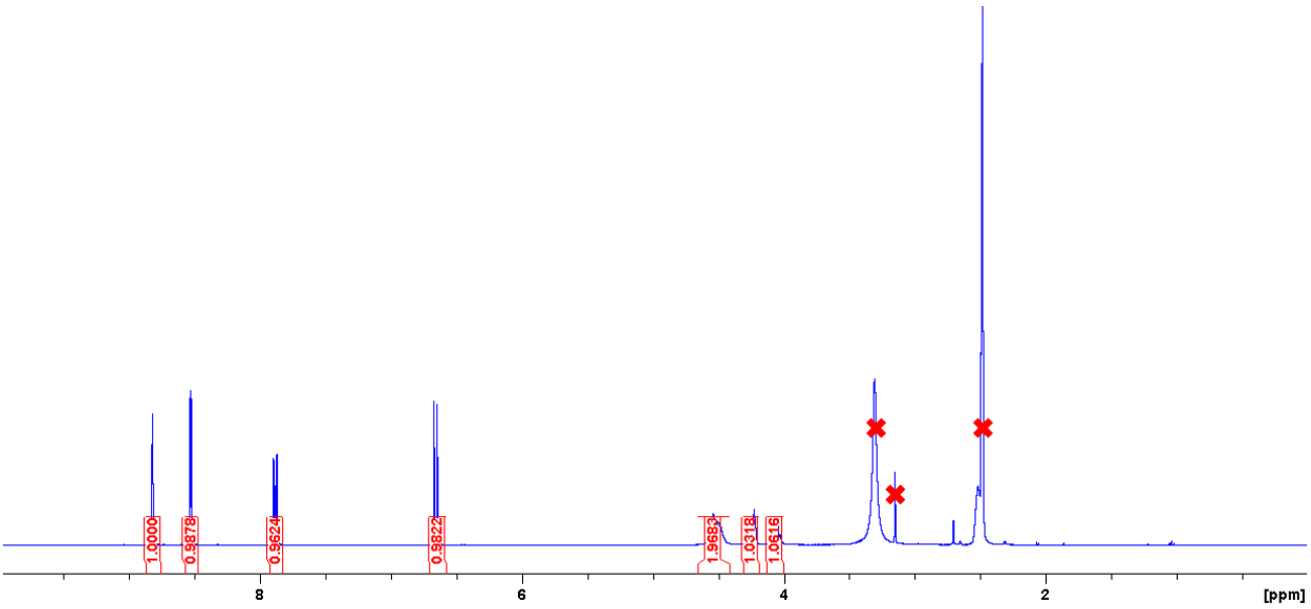

Figure S24. ^{1}H NMR of **2** with integrations. Solvent impurities of water (3.31 ppm), methanol (3.16 ppm), and DMSO (2.48 ppm) are marked with x.

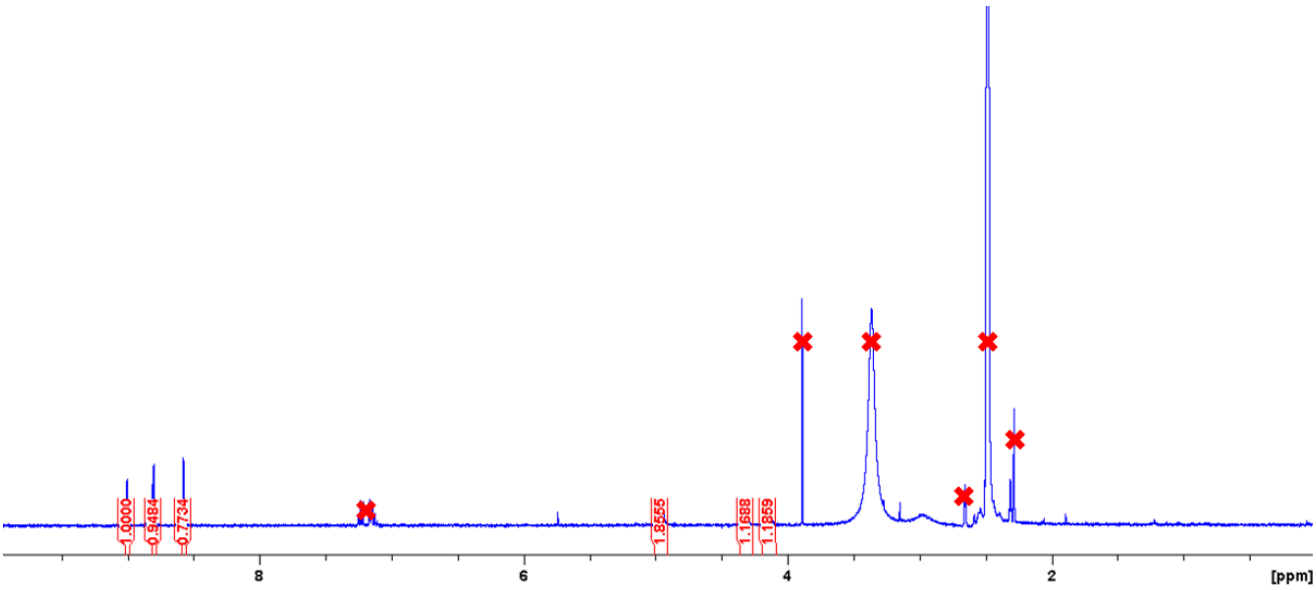

Figure S25. ^{1}H NMR of **3** with integrations. Solvent impurities of toluene (7.2 ppm, 2.29 ppm), methanol (3.89 ppm), water (3.36 ppm), and DMSO (2.48 ppm) are marked with x.

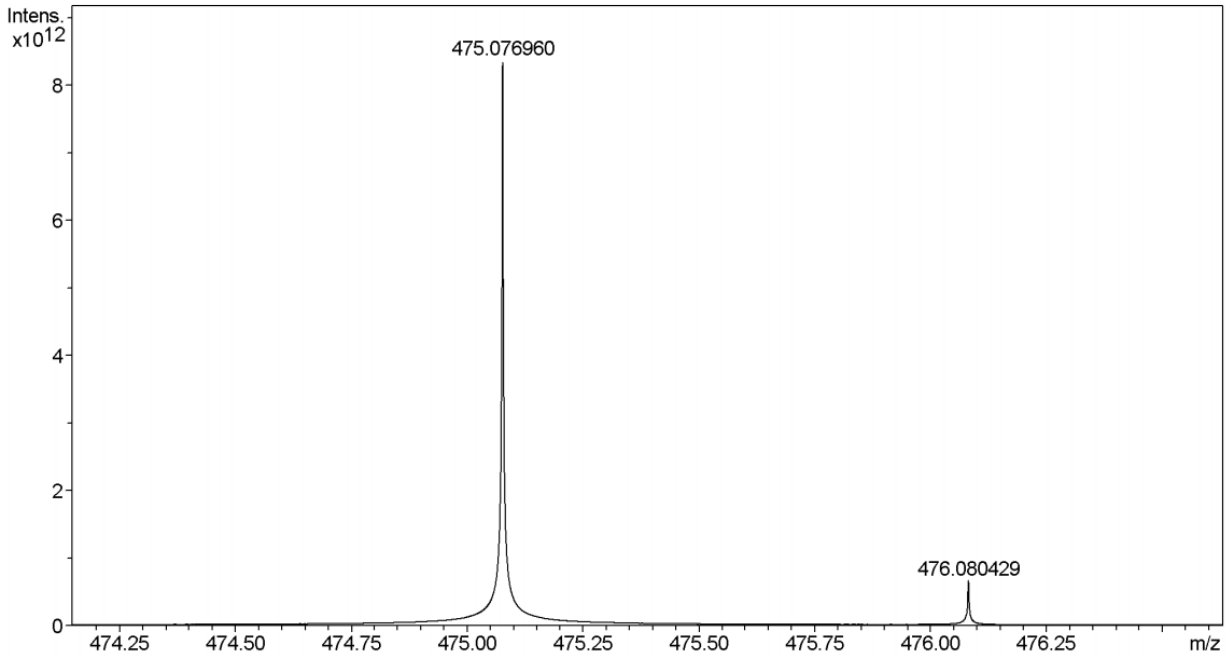

Figure S26. High-resolution mass spectrum of **2**.

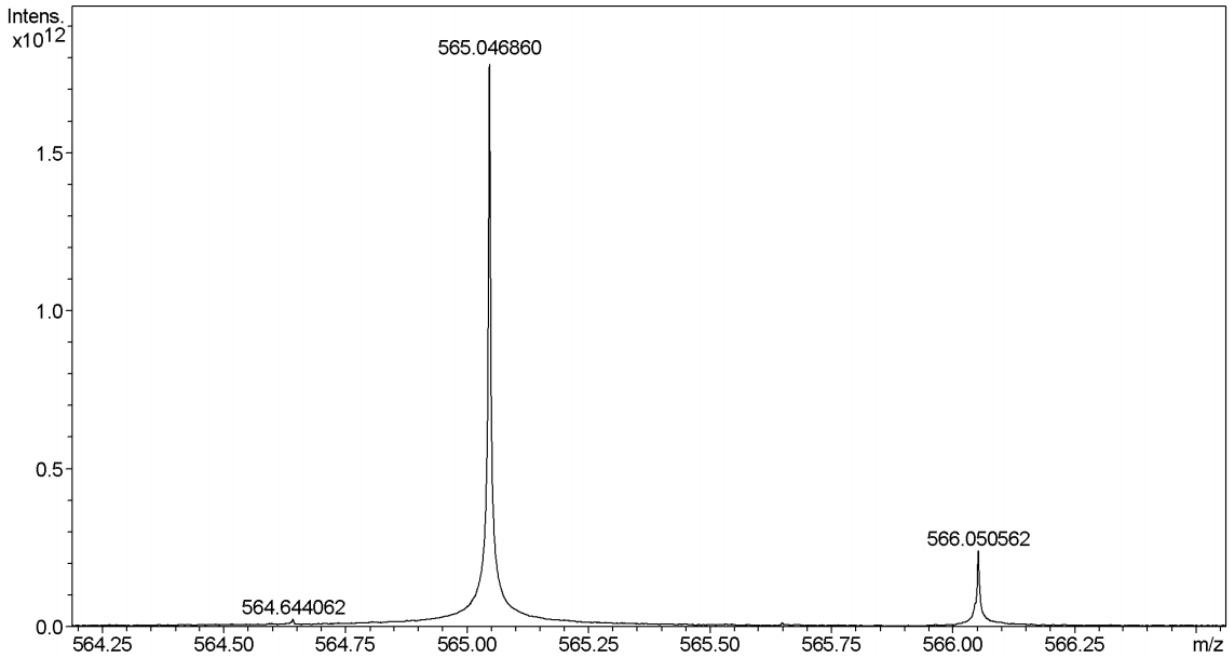

Figure S27. High-resolution mass spectrum of **3.**

Table S1. Crystal data and structure refinement for **2**.

Identification code	cwmwm10	
Empirical formula	C32 H36 B0.30 Co F5.39 N6 O6 P0.70	
Formula weight	786.97	
Temperature	100.0(5) K	
Wavelength	0.71073 Å	
Crystal system	monoclinic	
Space group	*C*2/*c*	
Unit cell dimensions	*a* = 13.6579(11) Å	α = 90°
	b = 18.1377(15) Å	β = 90.4907(18)°
	c = 13.7492(11) Å	γ = 90°
Volume	3405.9(5) Å^3	
Z	4	
Density (calculated)	1.535 Mg/m^3	
Absorption coefficient	0.620 mm^{-1}	
F(000)	1622	
Crystal color, morphology	pink-red, needle	
Crystal size	0.48 x 0.20 x 0.12 mm^3	
Theta range for data collection	1.867 to 36.406°	
Index ranges	$-22 \le h \le 22$, $-30 \le k \le 30$, $-22 \le l \le 22$	
Reflections collected	118185	
Independent reflections	8288 [*R*(int) = 0.0754]	
Observed reflections	6153	
Completeness to theta = 36.319°	100.0%	
Absorption correction	Multi-scan	
Max. and min. transmission	0.7471 and 0.6514	
Refinement method	Full-matrix least-squares on F^2	
Data / restraints / parameters	8288 / 51 / 278	
Goodness-of-fit on F^2	1.024	
Final *R* indices [*I*>2sigma(*I*)]	*R*1 = 0.0407, *wR*2 = 0.0980	
R indices (all data)	*R*1 = 0.0644, *wR*2 = 0.1093	
Largest diff. peak and hole	0.832 and -0.425 e.Å^{-3}	

Table S2. Bond lengths [Å] and angles [°] for **2**.

CO1-O(1)#1	1.8940(9)	C(6)-N(3)	1.4395(15)
CO1-O(1)	1.8940(9)	C(7)-C(8)	1.3692(17)
CO1-N(2)	1.9024(10)	C(7)-H(7)	0.9500
CO1-N(2)#1	1.9025(10)	C(8)-C(9)	1.4218(17)
CO1-N(1)	1.9600(11)	C(8)-H(8)	0.9500
CO1-N(1')	1.9600(11)	C(9)-O(1)	1.2967(14)
CO1-N(1)#1	1.9600(11)	N(3)-O(2)	1.2377(15)
CO1-N(1')#1	1.9600(11)	N(3)-O(3)	1.2422(14)
N(1)-C(1)	1.4908(17)	P(1)-F(1)#1	1.5921(15)
N(1)-H(1E)	0.9100	P(1)-F(1)	1.5921(15)
N(1)-H(1F)	0.9100	P(1)-F(3)	1.6020(12)
C(1)-C(2)	1.515(2)	P(1)-F(3)#1	1.6020(12)
C(1)-H(1A)	0.9900	P(1)-F(2)#1	1.6209(13)
C(1)-H(1B)	0.9900	P(1)-F(2)	1.6209(13)
C(2)-N(2)	1.4624(17)	B(1')-F(1')	1.365(7)
C(2)-H(2A)	0.9900	B(1')-F(3')	1.367(7)
C(2)-H(2B)	0.9900	B(1')-F(4')	1.368(7)
N(1')-C(1')	1.556(9)	B(1')-F(2')	1.369(7)
N(1')-H(1G)	0.9100	C(10)-C(11)	1.507(2)
N(1')-H(1H)	0.9100	C(10)-H(10A)	0.9800
C(1')-C(2')	1.503(13)	C(10)-H(10B)	0.9800
C(1')-H(1C)	0.9900	C(10)-H(10C)	0.9800
C(1')-H(1D)	0.9900	C(11)-C(12)	1.392(2)
C(2')-N(2)	1.589(11)	C(11)-C(16)	1.396(2)
C(2')-H(2C)	0.9900	C(12)-C(13)	1.384(2)
C(2')-H(2D)	0.9900	C(12)-H(12)	0.9500
N(2)-C(3)	1.2837(15)	C(13)-C(14)	1.388(3)
C(3)-C(4)	1.4385(17)	C(13)-H(13)	0.9500
C(3)-H(3)	0.9500	C(14)-C(15)	1.384(3)
C(4)-C(5)	1.4019(16)	C(14)-H(14)	0.9500
C(4)-C(9)	1.4323(16)	C(15)-C(16)	1.389(3)
C(5)-C(6)	1.3806(17)	C(15)-H(15)	0.9500
C(5)-H(5)	0.9500	C(16)-H(16)	0.9500
C(6)-C(7)	1.4055(17)	O(1)#1-CO1-O(1)	91.20(6)

O(1)#1-CO1-N(2)	87.49(4)	N(2)-C(2)-H(2A)	110.7
O(1)-CO1-N(2)	94.35(4)	C(1)-C(2)-H(2A)	110.7
O(1)#1-CO1-N(2)#1	94.35(4)	N(2)-C(2)-H(2B)	110.7
O(1)-CO1-N(2)#1	87.49(4)	C(1)-C(2)-H(2B)	110.7
N(2)-CO1-N(2)#1	177.37(6)	H(2A)-C(2)-H(2B)	108.8
O(1)#1-CO1-N(1)	87.51(4)	C(1')-N(1')-CO1	112.3(4)
O(1)-CO1-N(1)	178.66(4)	C(1')-N(1')-H(1G)	109.2
N(2)-CO1-N(1)	85.27(4)	CO1-N(1')-H(1G)	109.2
N(2)#1-CO1-N(1)	92.93(4)	C(1')-N(1')-H(1H)	109.2
O(1)#1-CO1-N(1')	87.51(4)	CO1-N(1')-H(1H)	109.2
O(1)-CO1-N(1')	178.66(4)	H(1G)-N(1')-H(1H)	107.9
N(2)-CO1-N(1')	85.27(4)	C(2')-C(1')-N(1')	102.3(7)
N(2)#1-CO1-N(1')	92.93(4)	C(2')-C(1')-H(1C)	111.3
O(1)#1-CO1-N(1)#1	178.67(4)	N(1')-C(1')-H(1C)	111.3
O(1)-CO1-N(1)#1	87.51(4)	C(2')-C(1')-H(1D)	111.3
N(2)-CO1-N(1)#1	92.93(4)	N(1')-C(1')-H(1D)	111.3
N(2)#1-CO1-N(1)#1	85.27(4)	H(1C)-C(1')-H(1D)	109.2
N(1)-CO1-N(1)#1	93.79(6)	C(1')-C(2')-N(2)	107.1(8)
O(1)#1-CO1-N(1')#1	178.67(4)	C(1')-C(2')-H(2C)	110.3
O(1)-CO1-N(1')#1	87.51(4)	N(2)-C(2')-H(2C)	110.3
N(2)-CO1-N(1')#1	92.93(4)	C(1')-C(2')-H(2D)	110.3
N(2)#1-CO1-N(1')#1	85.27(4)	N(2)-C(2')-H(2D)	110.3
N(1')-CO1-N(1')#1	93.79(6)	H(2C)-C(2')-H(2D)	108.6
C(1)-N(1)-CO1	107.93(8)	C(3)-N(2)-C(2)	120.15(10)
C(1)-N(1)-H(1E)	110.1	C(3)-N(2)-C(2')	118.0(4)
CO1-N(1)-H(1E)	110.1	C(3)-N(2)-CO1	126.59(9)
C(1)-N(1)-H(1F)	110.1	C(2)-N(2)-CO1	113.23(8)
CO1-N(1)-H(1F)	110.1	C(2')-N(2)-CO1	111.1(4)
H(1E)-N(1)-H(1F)	108.4	N(2)-C(3)-C(4)	124.25(10)
N(1)-C(1)-C(2)	107.04(11)	N(2)-C(3)-H(3)	117.9
N(1)-C(1)-H(1A)	110.3	C(4)-C(3)-H(3)	117.9
C(2)-C(1)-H(1A)	110.3	C(5)-C(4)-C(9)	119.90(11)
N(1)-C(1)-H(1B)	110.3	C(5)-C(4)-C(3)	117.27(10)
C(2)-C(1)-H(1B)	110.3	C(9)-C(4)-C(3)	122.68(10)
H(1A)-C(1)-H(1B)	108.6	C(6)-C(5)-C(4)	119.96(11)
N(2)-C(2)-C(1)	105.19(11)	C(6)-C(5)-H(5)	120.0

C(4)-C(5)-H(5)	120.0	F(3')-B(1')-F(2')	108.6(8)
C(5)-C(6)-C(7)	121.32(11)	F(4')-B(1')-F(2')	112.7(8)
C(5)-C(6)-N(3)	119.65(11)	C(11)-C(10)-H(10A)	109.5
C(7)-C(6)-N(3)	118.85(11)	C(11)-C(10)-H(10B)	109.5
C(8)-C(7)-C(6)	119.28(12)	H(10A)-C(10)-H(10B)	109.5
C(8)-C(7)-H(7)	120.4	C(11)-C(10)-H(10C)	109.5
C(6)-C(7)-H(7)	120.4	H(10A)-C(10)-H(10C)	109.5
C(7)-C(8)-C(9)	121.80(11)	H(10B)-C(10)-H(10C)	109.5
C(7)-C(8)-H(8)	119.1	C(12)-C(11)-C(16)	118.12(15)
C(9)-C(8)-H(8)	119.1	C(12)-C(11)-C(10)	121.24(14)
O(1)-C(9)-C(8)	117.51(10)	C(16)-C(11)-C(10)	120.63(15)
O(1)-C(9)-C(4)	124.76(11)	C(13)-C(12)-C(11)	121.18(15)
C(8)-C(9)-C(4)	117.72(10)	C(13)-C(12)-H(12)	119.4
C(9)-O(1)-CO1	126.10(8)	C(11)-C(12)-H(12)	119.4
O(2)-N(3)-O(3)	122.22(11)	C(12)-C(13)-C(14)	120.24(17)
O(2)-N(3)-C(6)	119.09(11)	C(12)-C(13)-H(13)	119.9
O(3)-N(3)-C(6)	118.67(11)	C(14)-C(13)-H(13)	119.9
F(1)#1-P(1)-F(1)	91.6(2)	C(15)-C(14)-C(13)	119.24(16)
F(1)#1-P(1)-F(3)	91.01(12)	C(15)-C(14)-H(14)	120.4
F(1)-P(1)-F(3)	90.89(13)	C(13)-C(14)-H(14)	120.4
F(1)#1-P(1)-F(3)#1	90.89(13)	C(14)-C(15)-C(16)	120.50(17)
F(1)-P(1)-F(3)#1	91.01(12)	C(14)-C(15)-H(15)	119.8
F(3)-P(1)-F(3)#1	177.28(13)	C(16)-C(15)-H(15)	119.8
F(1)#1-P(1)-F(2)#1	89.94(11)	C(15)-C(16)-C(11)	120.71(17)
F(1)-P(1)-F(2)#1	178.46(12)	C(15)-C(16)-H(16)	119.6
F(3)-P(1)-F(2)#1	88.82(7)	C(11)-C(16)-H(16)	119.6
F(3)#1-P(1)-F(2)#1	89.23(8)		
F(1)#1-P(1)-F(2)	178.46(12)		
F(1)-P(1)-F(2)	89.94(11)		
F(3)-P(1)-F(2)	89.23(8)		
F(3)#1-P(1)-F(2)	88.82(7)		
F(2)#1-P(1)-F(2)	88.55(10)		
F(1')-B(1')-F(3')	107.9(8)		
F(1')-B(1')-F(4')	109.0(9)		
F(3')-B(1')-F(4')	109.4(8)		
F(1')-B(1')-F(2')	109.1(9)		

Symmetry transformations used to generate equivalent atoms:
#1 -x+1,y,-z+3/2

Table S3. Crystal data and structure refinement for **3**.

Identification code	cwmwm08	
Empirical formula	C25 H26 B Co F4 N8 O10	
Formula weight	744.28	
Temperature	100.0(5) K	
Wavelength	0.71073 Å	
Crystal system	monoclinic	
Space group	*C*2/*c*	
Unit cell dimensions	*a* = 14.6690(16) Å	α = 90°
	b = 15.7386(17) Å	β = 99.389(2)°
	c = 12.9152(14) Å	γ = 90°
Volume	2941.8(6) Å^3	
Z	4	
Density (calculated)	1.680 Mg/m^3	
Absorption coefficient	0.681 mm^{-1}	
F(000)	1520	
Crystal color, morphology	pink-red, needle	
Crystal size	0.48 x 0.20 x 0.12 mm^3	
Theta range for data collection	1.912 to 38.792°	
Index ranges	$-25 \le h \le 25$, $-27 \le k \le 27$, $-22 \le l \le 22$	
Reflections collected	64770	
Independent reflections	8254 [*R*(int) = 0.0483]	
Observed reflections	6347	
Completeness to theta = 37.785°	99.7%	
Absorption correction	Multi-scan	
Max. and min. transmission	0.7476 and 0.6618	
Refinement method	Full-matrix least-squares on F^2	
Data / restraints / parameters	8254 / 6 / 251	
Goodness-of-fit on F^2	1.041	
Final *R* indices [*I*>2sigma(*I*)]	*R*1 = 0.0454, *wR*2 = 0.1181	
R indices (all data)	*R*1 = 0.0653, *wR*2 = 0.1288	
Largest diff. peak and hole	1.141 and -0.486 e.Å^{-3}	

Table S4. Bond lengths [Å] and angles [°] for **3**.

CO1-O(1)#1	1.8958(9)	B(1)-F(1)#2	1.3799(16)
CO1-O(1)	1.8959(9)	B(1)-F(2)	1.4040(15)
CO1-N(2)#1	1.9029(10)	B(1)-F(2)#2	1.4040(15)
CO1-N(2)	1.9029(10)	C(10)-C(11)	1.46(3)
CO1-N(1)	1.9540(10)	C(10)-H(10A)	0.9800
CO1-N(1)#1	1.9541(10)	C(10)-H(10B)	0.9800
N(1)-C(1)	1.4875(16)	C(10)-H(10C)	0.9800
N(1)-H(1C)	0.84(2)	C(11)-C(16)	1.340(18)
N(1)-H(1D)	0.916(19)	C(11)-C(12)	1.341(18)
C(1)-C(2)	1.5133(18)	C(12)-C(13)	1.49(3)
C(1)-H(1A)	0.9900	C(12)-H(12)	0.9500
C(1)-H(1B)	0.9900	C(13)-C(14)	1.40(2)
C(2)-N(2)	1.4790(15)	C(13)-H(13)	0.9500
C(2)-H(2A)	0.9900	C(14)-C(15)	1.41(2)
C(2)-H(2B)	0.9900	C(14)-H(14)	0.9500
N(2)-C(3)	1.2818(15)	C(15)-C(16)	1.49(3)
C(3)-C(4)	1.4547(16)	C(15)-H(15)	0.9500
C(3)-H(3)	0.9500	C(16)-H(16)	0.9500
C(4)-C(5)	1.3952(16)	O(1)#1-CO1-O(1)	89.61(6)
C(4)-C(9)	1.4332(16)	O(1)#1-CO1-N(2)#1	94.05(4)
C(5)-C(6)	1.3886(17)	O(1)-CO1-N(2)#1	87.24(4)
C(5)-H(5)	0.9500	O(1)#1-CO1-N(2)	87.24(4)
C(6)-C(7)	1.3852(18)	O(1)-CO1-N(2)	94.05(4)
C(6)-N(3)	1.4483(16)	N(2)#1-CO1-N(2)	178.18(6)
C(7)-C(8)	1.3770(17)	O(1)#1-CO1-N(1)	88.08(4)
C(7)-H(7)	0.9500	O(1)-CO1-N(1)	177.62(4)
C(8)-C(9)	1.4302(16)	N(2)#1-CO1-N(1)	93.52(4)
C(8)-N(4)	1.4607(16)	N(2)-CO1-N(1)	85.24(4)
C(9)-O(1)	1.2834(14)	O(1)#1-CO1-N(1)#1	177.62(4)
N(3)-O(2)	1.2202(16)	O(1)-CO1-N(1)#1	88.09(4)
N(3)-O(3)	1.2370(16)	N(2)#1-CO1-N(1)#1	85.25(4)
N(4)-O(5)	1.2206(15)	N(2)-CO1-N(1)#1	93.52(4)
N(4)-O(4)	1.2376(15)	N(1)-CO1-N(1)#1	94.23(6)
B(1)-F(1)	1.3798(16)	C(1)-N(1)-CO1	107.20(7)

C(1)-N(1)-H(1C)	109.3(15)	C(7)-C(8)-N(4)	116.44(11)
CO1-N(1)-H(1C)	110.8(15)	C(9)-C(8)-N(4)	120.04(10)
C(1)-N(1)-H(1D)	111.0(12)	O(1)-C(9)-C(8)	119.64(10)
CO1-N(1)-H(1D)	113.4(12)	O(1)-C(9)-C(4)	124.91(10)
H(1C)-N(1)-H(1D)	105.1(19)	C(8)-C(9)-C(4)	115.44(10)
N(1)-C(1)-C(2)	106.24(9)	C(9)-O(1)-CO1	126.86(7)
N(1)-C(1)-H(1A)	110.5	O(2)-N(3)-O(3)	123.08(12)
C(2)-C(1)-H(1A)	110.5	O(2)-N(3)-C(6)	119.10(11)
N(1)-C(1)-H(1B)	110.5	O(3)-N(3)-C(6)	117.80(11)
C(2)-C(1)-H(1B)	110.5	O(5)-N(4)-O(4)	124.15(12)
H(1A)-C(1)-H(1B)	108.7	O(5)-N(4)-C(8)	119.51(11)
N(2)-C(2)-C(1)	106.35(9)	O(4)-N(4)-C(8)	116.34(11)
N(2)-C(2)-H(2A)	110.5	F(1)-B(1)-F(1)#2	108.82(17)
C(1)-C(2)-H(2A)	110.5	F(1)-B(1)-F(2)	110.13(6)
N(2)-C(2)-H(2B)	110.5	F(1)#2-B(1)-F(2)	110.41(7)
C(1)-C(2)-H(2B)	110.5	F(1)-B(1)-F(2)#2	110.41(7)
H(2A)-C(2)-H(2B)	108.7	F(1)#2-B(1)-F(2)#2	110.13(6)
C(3)-N(2)-C(2)	119.62(10)	F(2)-B(1)-F(2)#2	106.93(16)
C(3)-N(2)-CO1	127.02(8)	C(11)-C(10)-H(10A)	109.5
C(2)-N(2)-CO1	113.31(7)	C(11)-C(10)-H(10B)	109.5
N(2)-C(3)-C(4)	124.33(10)	H(10A)-C(10)-H(10B)	109.5
N(2)-C(3)-H(3)	117.8	C(11)-C(10)-H(10C)	109.5
C(4)-C(3)-H(3)	117.8	H(10A)-C(10)-H(10C)	109.5
C(5)-C(4)-C(9)	121.13(10)	H(10B)-C(10)-H(10C)	109.5
C(5)-C(4)-C(3)	117.08(10)	C(16)-C(11)-C(12)	124(3)
C(9)-C(4)-C(3)	121.74(10)	C(16)-C(11)-C(10)	118.0(14)
C(6)-C(5)-C(4)	119.73(11)	C(12)-C(11)-C(10)	117.6(14)
C(6)-C(5)-H(5)	120.1	C(11)-C(12)-C(13)	117.7(15)
C(4)-C(5)-H(5)	120.1	C(11)-C(12)-H(12)	121.2
C(7)-C(6)-C(5)	121.78(11)	C(13)-C(12)-H(12)	121.2
C(7)-C(6)-N(3)	118.39(11)	C(14)-C(13)-C(12)	122.1(14)
C(5)-C(6)-N(3)	119.72(11)	C(14)-C(13)-H(13)	119.0
C(8)-C(7)-C(6)	118.36(11)	C(12)-C(13)-H(13)	119.0
C(8)-C(7)-H(7)	120.8	C(13)-C(14)-C(15)	116(2)
C(6)-C(7)-H(7)	120.8	C(13)-C(14)-H(14)	122.1
C(7)-C(8)-C(9)	123.52(11)	C(15)-C(14)-H(14)	122.1

C(14)-C(15)-C(16)	121.5(14)	C(11)-C(16)-H(16)	120.9
C(14)-C(15)-H(15)	119.3	C(15)-C(16)-H(16)	120.9
C(16)-C(15)-H(15)	119.3		
C(11)-C(16)-C(15)	118.1(15)		

Symmetry transformations used to generate equivalent atoms:
#1 -x+1,y,-z+1/2 #2 -x,y,-z+1/2

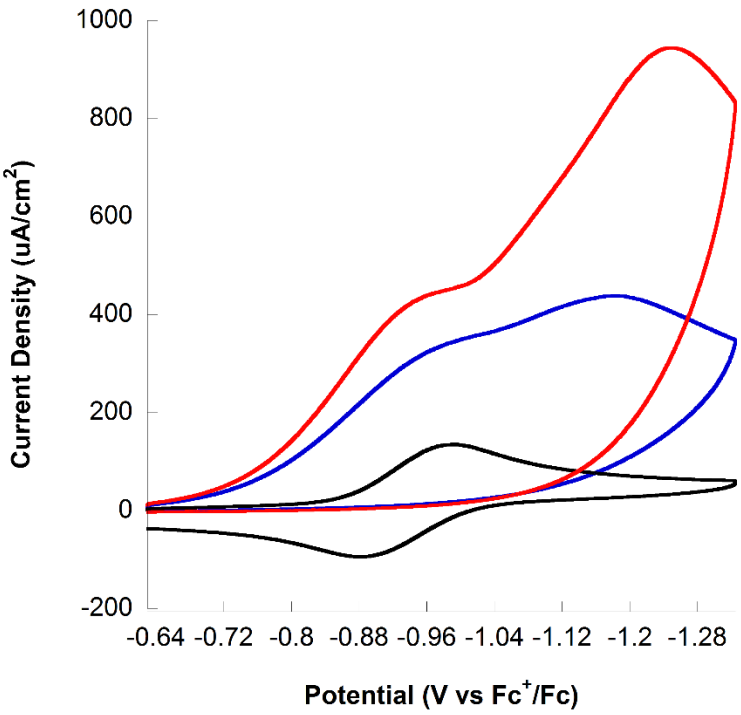

Figure S28. CV of 0 mM (Black), 4.4 mM (Blue), and 8.8 mM (Red) of tosic acid with 0.5 mg of **2** and 0.1 M $TBAPF_6$ in CH_3CN at ν = 200 mV/s.

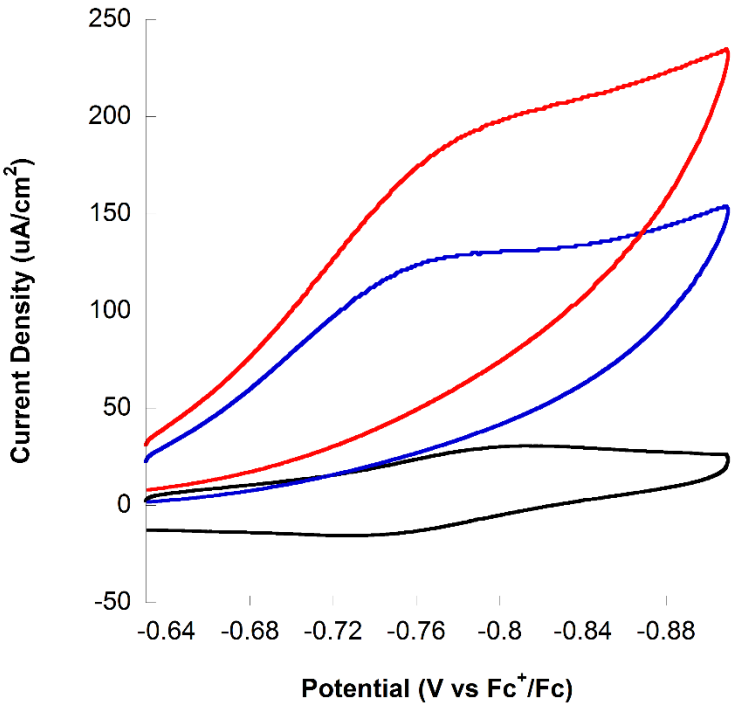

Figure S29. CV of 0 mM (Black), 4.4 mM (Blue), and 8.8 mM (Red) of tosic acid with 0.5 mg of **3** and 0.1 M $TBAPF_6$ in CH_3CN at ν = 200 mV/s.

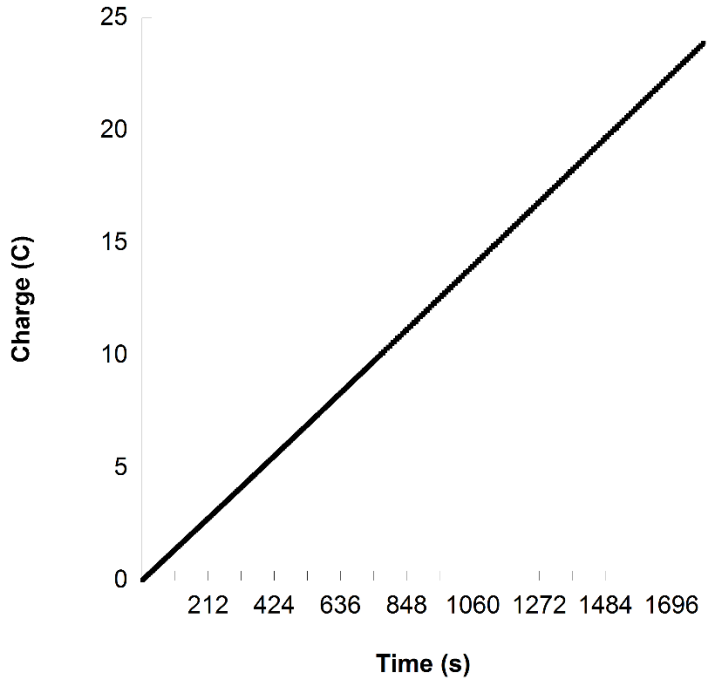

Figure S30. Bulk Electrolysis of 0.5 mg (0.001 mmol) of **2** in a 0.1 M solution of $TBAPF_6$ in CH_3CN with 65 mM TFA. The potential was held at -1.2 V vs. Fc^+/Fc for 1800 seconds resulting in a charge of 24 C, corresponding to a TON of 120 after 30 minutes. A GC of the headspace gases corresponded to a faradaic yield of 98%.

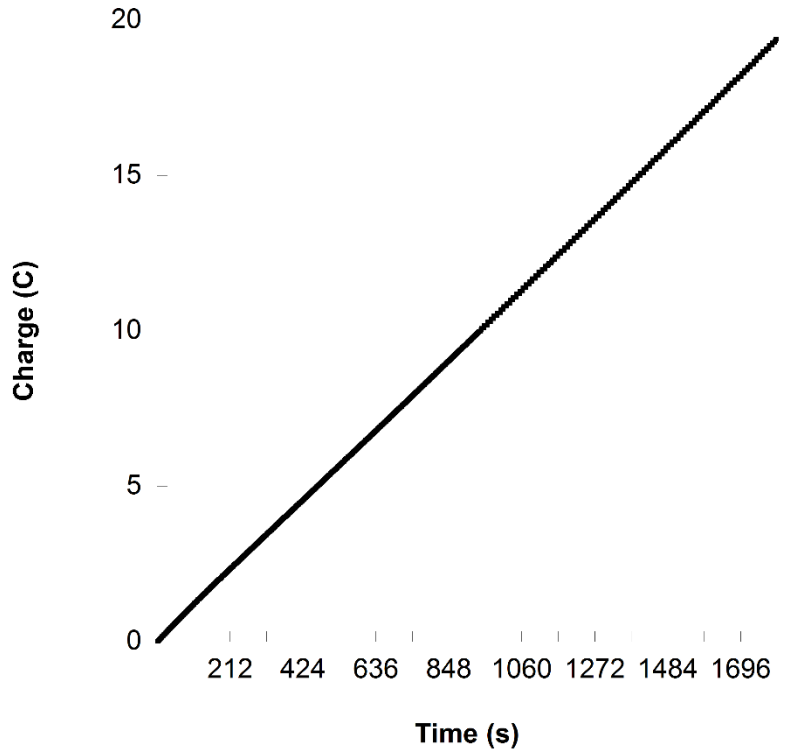

Figure S31. Bulk Electrolysis of 0.5 mg (8.85 x 10^{-4} mol) **3** in a 0.1 M solution of $TBAPF_6$ in CH_3CN with 65 mM TFA. The potential was held at -1.0 V vs. Fc^+/Fc for 1800 seconds resulting in a charge of 19 C, corresponding to a TON of 112 after 30 minutes. A GC of the headspace gases corresponded to a faradaic yield of 98%.

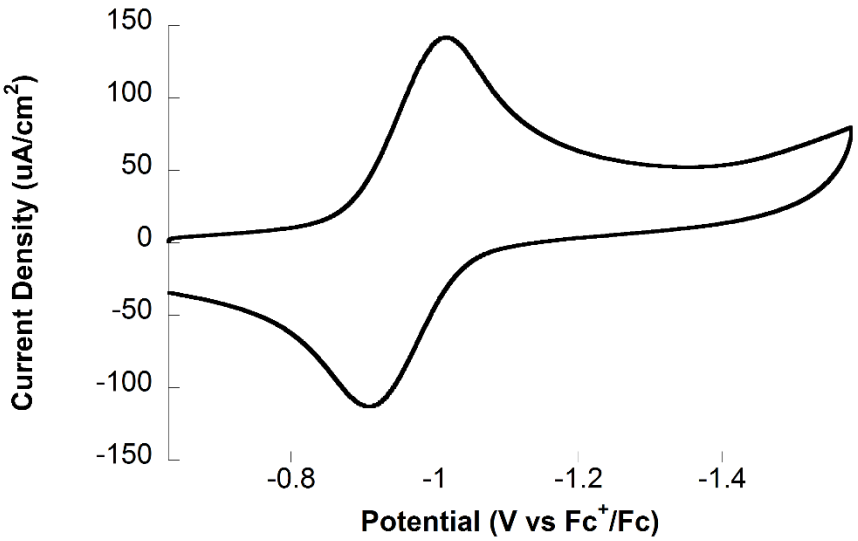

Figure S32. CV of 1 mg of **2** in CH_3CN with 0.1 M $TBAPF_6$.

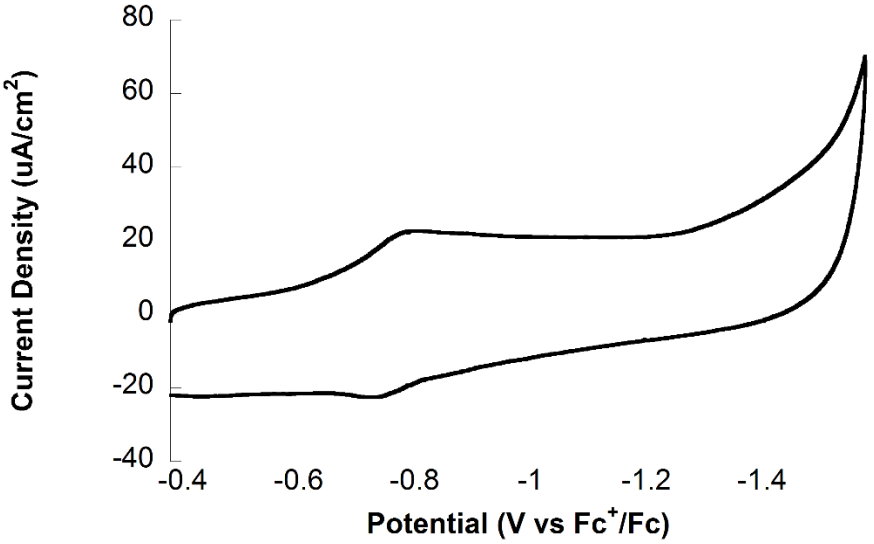

Figure S33. CV of 0.5 mg of **3** in CH_3CN with 0.1 M $TBAPF_6$.

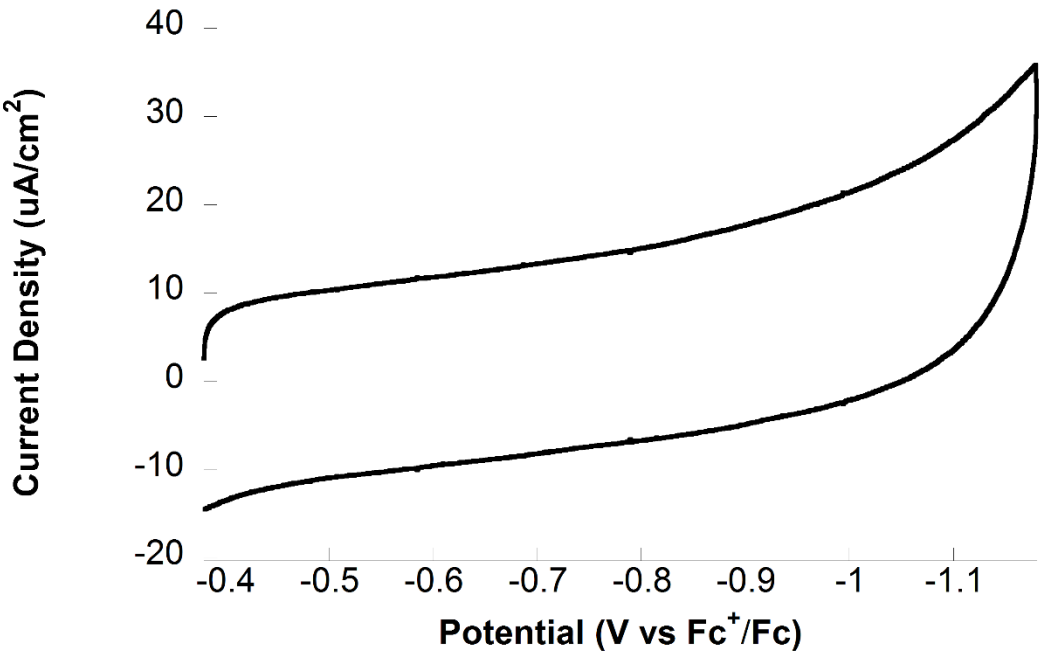

Figure S34. CV of electrodes used for bulk electrolysis of **2** in CH_3CN with 13.3 mM TFA (under condition outlined in Figure S31). The electrodes were rinsed with CH_3CN but not polished and a CV was obtained in CH_3CN with 0.1 M $TBAPF_6$ and 13.3 mM TFA. No catalytic film is observed.

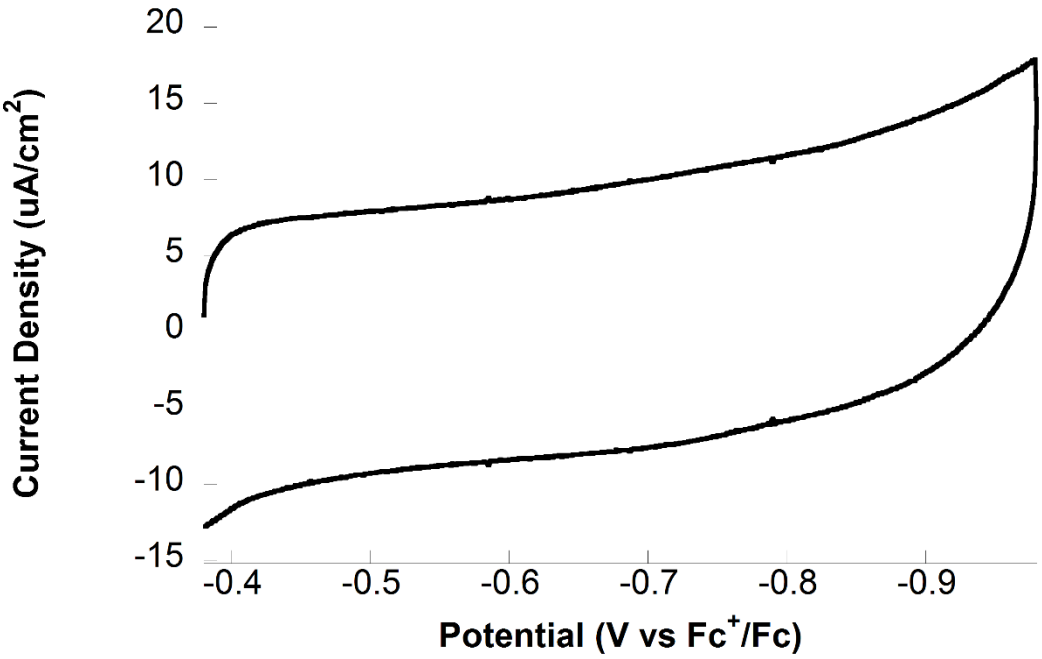

Figure S35. CV of electrodes used for bulk electrolysis of **3** in CH_3CN with 13.3 mM TFA (under condition outlined in Figure S32). The electrodes were rinsed with CH_3CN but not polished and a CV was obtained in CH_3CN with 0.1 M $TBAPF_6$ and 13.3 mM TFA. No catalytic film is observed.

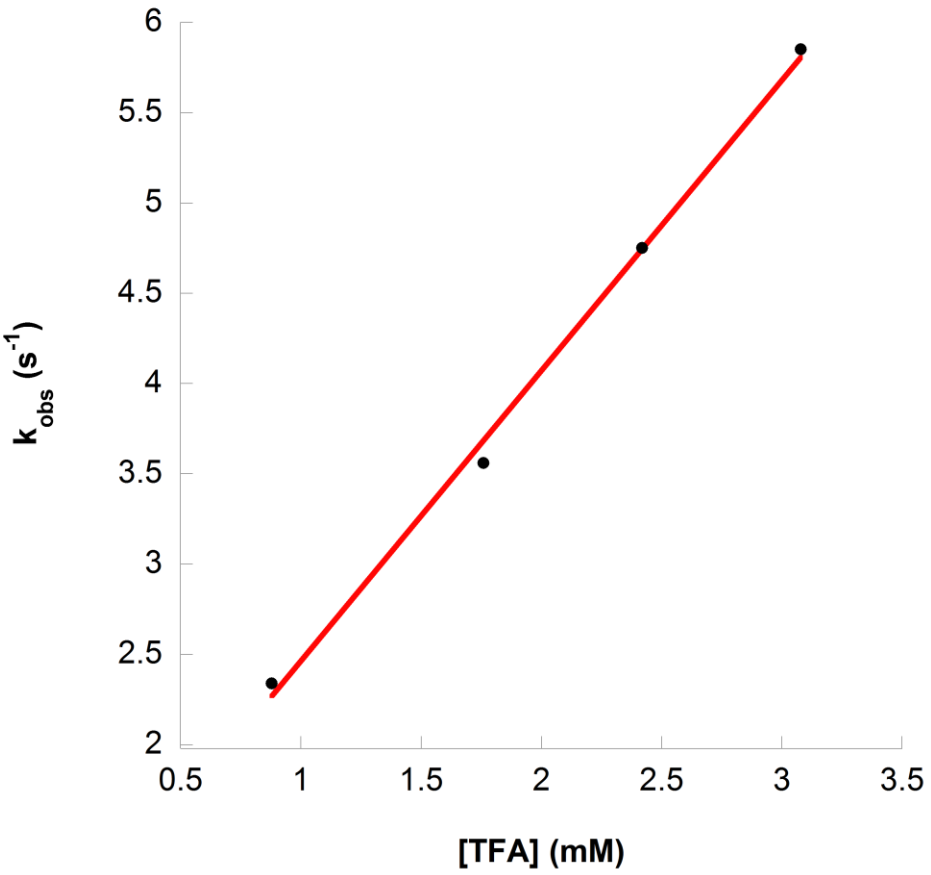

Figure S36. The k_{obs} vs. [H^+] for CVs of 0.5 mg of **2** in CH_3CN with 0.1 M $TBAPF_6$ upon addition of 0.88 mM, 1.76 mM, 2.42 mM, and 3.08 mM TFA at v = 200 mV/s. R^2= 0.99.

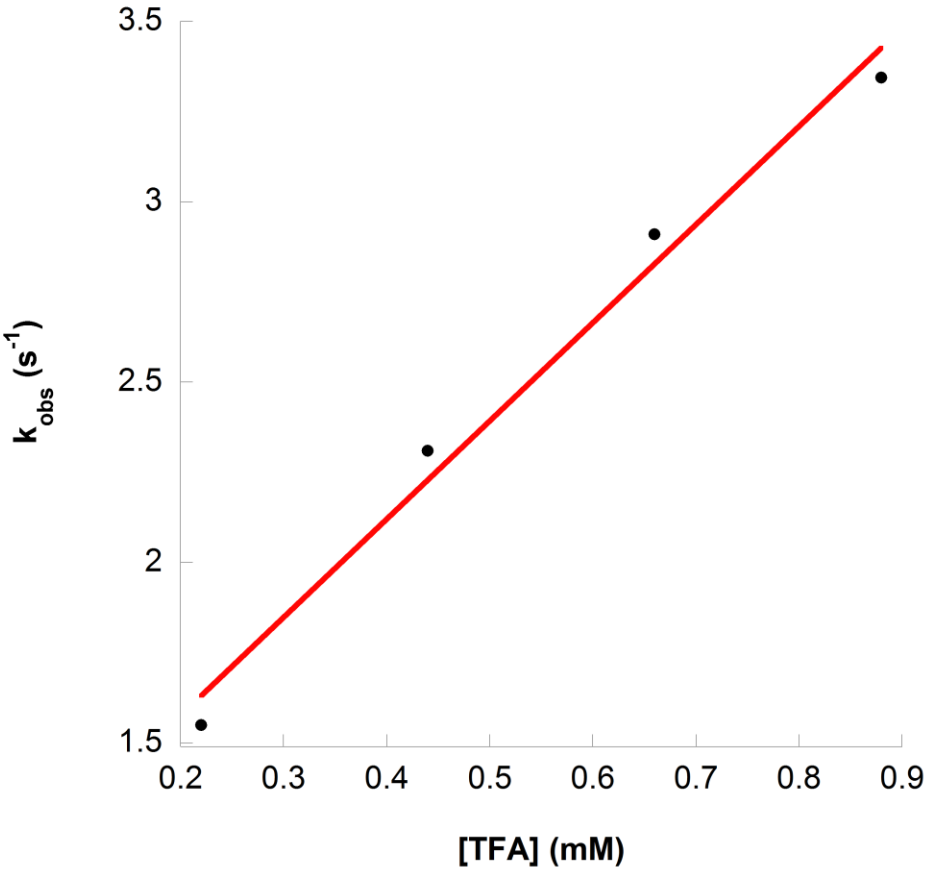

Figure S37. The k_{obs} vs. [H^+] for CVs of 0.5 mg of **3** in CH_3CN with 0.1 M $TBAPF_6$ upon addition of 0.22 mM, 0.44 mM, 0.66 mM, and 0.88 mM TFA at v = 200 mV/s. R^2= 0.99.

References

(1) Connor, G, Mayer, K, Tribble, C., and McNamara, W. *Inorg. Chem.* **2014**, 53 (11), 5408-5410. (b) Hartley, C.L., DiRisio, Ryan J., Chang, T.C., Zhang, W., & McNamara, W. R. *Polyhedron*, **2016**, 114, 133-137. (c) Cavell, A. C.; Hartley, C. L.; Liu, D.; Tribble, C. S.; McNamara, W. R. (2015) *Inorg. Chem*., **2015**, 54(7), 3325-3330. (d) Nicholson, R. S.; Shain, I. *Anal. Chem*. **1964**, 36, 706-723. (e) Bard, A. J.; Faulkner, L. R. Electrochemical Methods: Fundamentals and Applications, 2nd ed.; John Wiley & Sons: New York, 2001. (f) Saveant, J. M.; Vianello, E. *Electrochim. Acta*., **1965**, 10, 905-920. (g) Saveant, J. M.; Vianello, E. *Electrochim. Acta*., **1967**, 12, 629-646.
(2) Elgrishi, N., Chambers, M., & Fontecave, M. *Chem. Sci.*, **2015**, 6, 2522
(3) Rountree, E., Mccarthy, B., Eisenhart, T., & Dempsey, J. *Inorg. Chem*., **2014**, 53(19), 9983-10002.
(4) Costentin, C., Drouet, S., Robert, M., & Savéant, J. *J. Am. Chem. Soc.*, **2012**, 134(27), 11235-42.
(5) Wiedner, E. S., Bullock, R. M. *J. Am. Chem. Soc.*, **2016**, 138, 8309-8318.